

DEVELOPMENT OF FOIL THRUST BEARING TEST RIG

by

ROHIT HARISHCHANDRA YADAV

Presented to the Faculty of the Graduate School of  
The University of Texas at Arlington in Partial Fulfillment  
of the Requirements  
for the Degree of

MASTER OF SCIENCE IN MECHANICAL ENGINEERING

THE UNIVERSITY OF TEXAS AT ARLINGTON

MAY 2013

Copyright © by Rohit Harishchandra Yadav 2013

All Rights Reserved



## Acknowledgements

I sincerely thank my committee chair, Dr. Daejong Kim for his guidance, and support throughout the course of research. I would also like to thank Dr. Nomura and Dr. Bo Wang for serving as committee member.

I would like to express my gratitude to Kermit Beird and Sam Williams from machine shop for helping me at each stage in fabrication and assembly of test setup. I would like to thank my colleagues and friends in Microturbomachinery and Energy Systems Lab for their help and support.

And last but not the least, I would thank my family and friends for their love and support for all these years.

May 08, 2013

## Abstract

### DEVELOPMENT OF FOIL THRUST BEARING TEST RIG

Rohit Harishchandra Yadav, MS  
The University of Texas at Arlington, 2013

Supervising Professor: Daejong Kim

Oil lubricated bearings have been widely used in variety of turbo machinery, though it has its own limitations such as thermal degradation of oil over temperature, complicated oil lubrication system and their maintenance. Commercial application of the air foil bearing (AFB) in Microturbomachinery have been acknowledged. Microturbomachinery term is used in applications with shaft power less than 1000KW and shaft diameter less than 100mm. Microturbomachinery has demanded light weighted, compact, extreme temperature and high speed operation. DN number for oil lubricated bearings and rolling element bearings is very less when compared to foil bearings. Absence of external pressurizing and lubricating system makes the system light and compact. Simple construction, low friction drag and reliability at high speed operations are few more advantages of the foil bearings. With all these advantages, foil bearings appears to be the one of the most effective techniques for Microturbomachinery. With the relentless demand for machines capable of operating at greatest speeds, high power densities and temperatures, foil gas bearings represent an enabling technology for advanced oil free system. While air foil journal bearings have been advanced significantly in past decades, very few literature data are available and not much experimental work has been conducted on foil thrust bearings.

There is comparatively less information on air foil thrust bearings due to challenges in design, manufacturing and assembly. This research focuses on development of foil gas thrust bearing test rig which will operate at high temperature and speed. The test rig developed is equipped with thermocouple, optical probe, load cell which provides temperature, axial load, torque and high speed data by using NI labview. Design, manufacturing and assembly of air foil thrust bearing are detailed. The test rig has a push/pull mechanism which makes the stiffness measurement much easier. By evaluating parameters such as load capacity, steady state temperature, structural stiffness, and start stop friction torque will help to enhance the performance of the air foil thrust bearing.

## Table of Contents

Acknowledgements.....	iii
Abstract .....	iv
List of Illustrations .....	viii
List of Tables .....	x
Nomenclature .....	xi
Chapter 1 Introduction.....	1
1.1 Magnetic bearings.....	1
1.2 Air foil journal bearing.....	2
1.2.1 Principle of Operation:.....	3
1.3 Air Foil Thrust Bearing.....	4
1.3.1 Principle of Operation:.....	5
1.4 Motivation for studying Air foil thrust bearings.....	5
Chapter 2 Literature Review .....	7
2.1 Factors influencing the performance of foil gas thrust bearing.....	7
2.2 Performance prediction of hybrid air foil thrust bearings.....	9
2.3 Gas foil thrust bearing performance and its influencing factors.....	11
2.4 High Performance Foil Thrust Bearing Test Rig Developed.....	13
Chapter 3 Research Objective.....	16
Chapter 4 Description of Test Rig.....	17
4.1 10 KW Electric Motor.....	18
4.2 Bearing Housing.....	19
4.3 Manufacturing of journal bearing .....	21
4.4 Manufacturing of thrust bearing .....	24
4.5 Test housing .....	37

4.6	Instrumentation .....	40
4.6.1	Temperature Measurement .....	40
4.6.2	Pressure measurement .....	41
4.6.3	Vibration measurement .....	42
4.6.4	Stiffness and runner displacement measurement.....	44
4.6.5	Torque measurement.....	45
Chapter 5	Results and Conclusion.....	48
5.1	Future Work .....	52
Appendix A	Proximity Calibration to measure Stiffness.....	53
Bibliography.....		57
Biographical Information.....		58

## List of Illustrations

Figure 1-1 Magnetic bearing.....	2
Figure 1-2 Schematic of Air Foil Journal Bearing .....	3
Figure 1-3 Air Foil Thrust Bearing image from [1].....	4
Figure 2-1 Effect of cooling air flow on load capacity, image from [3] .....	8
Figure 2-2 Effect of surface roughness on load capacity, image from [3].....	9
Figure 2-3 Hybrid Air foil thrust bearing, image from [4] .....	10
Figure 2-4 Thrust bearing configuration. ....	12
Figure 2-5 Foil Thrust Bearing Rig, image from [6].....	14
Figure 2-6 Solid Model of Thrust Bearing Rig, image from [6] .....	14
Figure 4-1 10 KW Electric motor.....	18
Figure 4-2 Solid Model of Cross Sectional Bearing Housing .....	19
Figure 4-3 Temperature and Pressure Sensor .....	21
Figure 4-4 Bump foil forming jig.....	22
Figure 4-5 Bump foils after hydraulic press .....	23
Figure 4-6 Assembly of journal bearing .....	24
Figure 4-7 Base plate for thrust bearing.....	25
Figure 4-8 Bump foil Blanks .....	26
Figure 4-9 Bump foil forming jig.....	27
Figure 4-10 Bump foils .....	28
Figure 4-11 Prototype bearing with one top foil removed image from [1] .....	29
Figure 4-12 Radially arranged Bump foils image from [8].....	30
Figure 4-13 Top foil jig.....	31
Figure 4-14 Rayleigh Step top foil.....	31
Figure 4-15 All the parts to assemble thrust bearing .....	32



Figure 4-16 Rayleigh Step Bearing.....	33
Figure 4-17 Bump foils after removal of 2 strips from each sector .....	34
Figure 4-18 Top foil for Bearing B.....	35
Figure 4-19 Taper flat thrust foil bearing. ....	36
Figure 4-20 Solid Model of a Test Housing. ....	37
Figure 4-21 Push Pull Mechanism .....	38
Figure 4-22 Test Rig Assembly .....	40
Figure 4-23 Attached Thermocouple at the Back Plate .....	41
Figure 4-24 Temperature and Pressure VI.....	42
Figure 4-25 Proximity Sensor Connectors .....	43
Figure 4-26 NI USB 4432 DAQ.....	43
Figure 4-27 Vibration measurement VI .....	44
Figure 4-28 Torque Rod attached to shaft .....	46
Figure 4-29 Torque and Load Measurement VI .....	47
Figure 5-1 Structural Stiffness assembly .....	48
Figure 5-2 Stiffness Plot with 0.008" shim.....	49
Figure 5-3 Stiffness plot without shim. ....	49
Figure 5-4 Torque Graph.....	50
Figure 5-5 Axial load Graph.....	50
Figure 5-6 Temperature Graph.....	51
Figure 5-7 Pressure Profile.....	51

## List of Tables

Table 1-1 Comparison between different types of bearings.....	5
Table 4-1 Detail Components of Bearing Housing .....	19
Table 4-2 Components of Test Housing .....	37
Table 4-3 Detailed Components of Push Pull Mechanism.....	39

## Nomenclature

$p$	Absolute pressure within fluid film
$C$	Nominal bearing clearance in [ $m$ ]
$h$	Local fluid film thickness in [ $m$ ]
$H$	Non-dimensionalized film thickness
$P_a$	Atmospheric pressure [ $N / m^2$ ]
$R$	Bearing Radius [ $m$ ]
$\mu$	Air dynamic viscosity [ $N \cdot s / m^2$ ]
$W_o$	Reference Load [ $N$ ]

## Chapter 1

### Introduction

For years, oil lubricated bearings have been widely used in variety of turbomachinery, but they have their own drawbacks such as thermal degradation of oil over temperature, complicated oil lubrication systems and their maintenance. Microturbomachinery (shaft power less than 1000kW and shaft diameter less than 100mm from definition by Gas Turbine Institute) has gained interest due to its very high power to weight ratio, high operating speeds and can run on a wide variety of fuels. Microturbomachinery has demanded light weighted compact and even extreme temperature operations in some applications. However, while using oil lubricated bearings or rolling element bearings, microturbomachinerics are restricted to meet the desired requirements as oil lubricated bearings requires an external pressurizing unit which in turn makes the system much heavier and less compact. Also, oil lubricated bearings have a complex lubrication circuit to carry away excess heat and contaminants. Rolling element bearings have DN (diameter in mm and speed in rpm) number limit of nearly 1-2million, oil lubricated bearings have DN number of nearly 1million and magnetic bearings have DN number of nearly 3~4 million. Hence, oil lubricated bearings or rolling element bearings are not good in Microturbomachinery applications.

#### 1.1 Magnetic bearings

Figure 1-1 shows a magnetic bearing arrangement, which uses the principle of electromagnetism. The rotor is lifted off through the attractive electromagnetic forces produced by the coils placed around it in the stator. A position sensor helps to maintain the orbit of the rotor, which provides a feedback signal to the controller placing the rotor in the desired orbit and position. Magnetic bearings have high dynamic stiffness and damping.

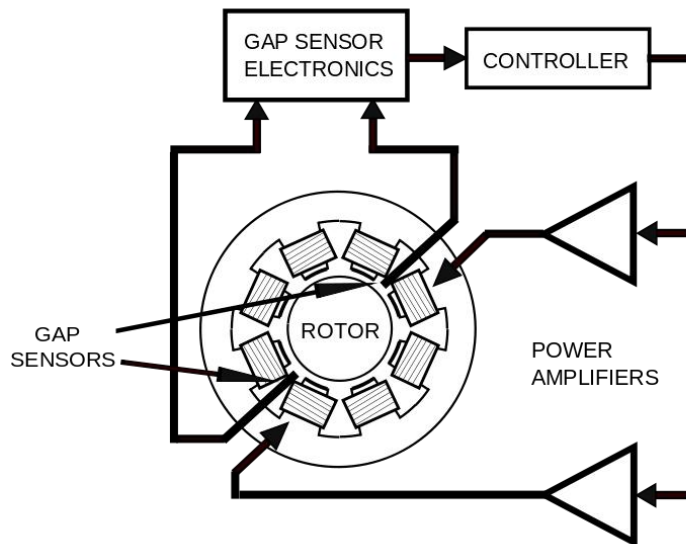


Figure 1-1 Magnetic bearing

## 1.2 Air foil journal bearing

Foil bearings are compliant, self acting hydrodynamic fluid film bearings uses air as lubricant which is not degraded by extreme temperatures. Figure 1-2 shows a schematic of air foil journal bearing. Air foil journal bearings comprises of a shaft which rotates in a bearing sleeve, the smooth sheet metal foil called as top foil acts as a bearing surface and is supported by series of corrugated bump foils which acts as a spring to give compliance to the bearing. The hydrodynamic pressure is built between the small gap between rotating shaft surface and top foil surface. The surface of the top foil is usually coated with solid lubricants to reduce the start-stop friction. Fixed end of top foil is called trailing edge and the free end is called leading edge. The journal rotates from leading edge to trailing edge i.e. free end to fixed end. The compliance structure also accommodates rotor centrifugal growth, thermal growth and misalignment. The underlying corrugated bump foil structure provides a tunable structural stiffness and

coulomb type damping, which is generated by relative motion between the bump foils and top foils. The structural stiffness of the bump foil is typically controlled by bump geometry and material. Typically, super alloy like nickel chromium alloy trademarked as Inconel is used for bump foil and top foil.

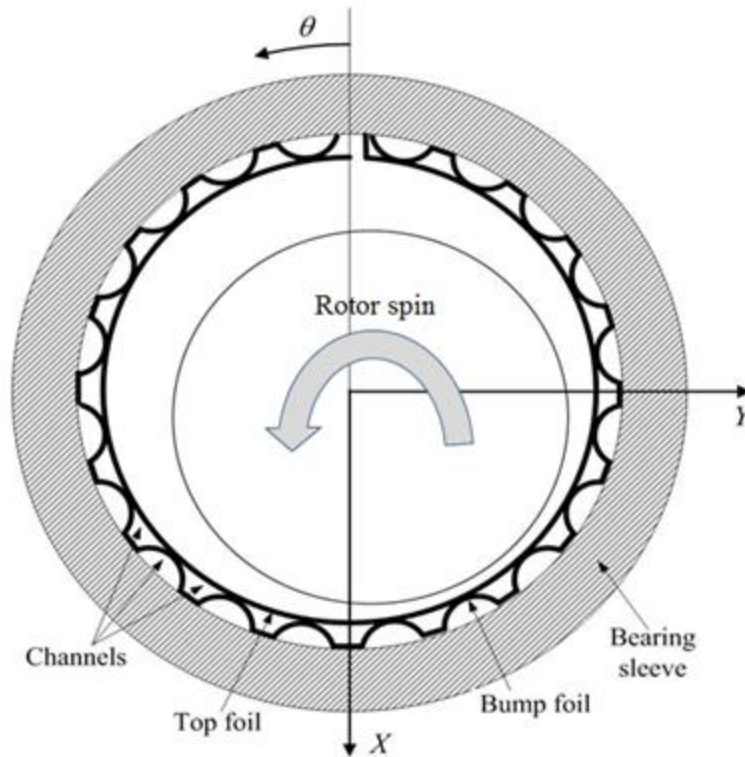


Figure 1-2 Schematic of Air Foil Journal Bearing

### 1.2.1 Principle of Operation:

Initial radial clearance creates the wedge-shaped void when rotor is at rest. The viscous pumping of the rotating shaft drags the ambient air into a converging wedge between the rotating shaft and non rotating surfaces. Hydrodynamic pressure begins to develop in the wedge as journal starts rotating resulting in formation of hydrodynamic film. The underlying compliant structure is self acting in accordance to the change in hydrodynamic pressure. Gradually the contact area between journal and top foil is reduced, until the

rotor reaches its lift-off speed where the rotor is completely air borne and solely supported by hydrodynamic film. The capability of self adjusting of compliant bearing surface can accommodate minor thermal growth and centrifugal growth of the rotor.

### 1.3 Air Foil Thrust Bearing

Figure 1-3 shows schematic of air foil thrust bearing. Air foil thrust bearings are self-acting compliant surface hydrodynamic bearing which operates on a thin lubricating gas film. Foil thrust bearing is made of three main components; back plate which serves as a base to the bearing, bumps foil and top foils. Air foil thrust bearing is divided circumferentially into number of sectors called pads. Each pad comprises of bump foils and top foil. The bump foils creates the spring like characteristics of the bearing. The top foil provides a smooth surface for the gas film to develop hydrodynamic pressure. The direction of rotation in thrust foil bearing is from fixed end to free end.

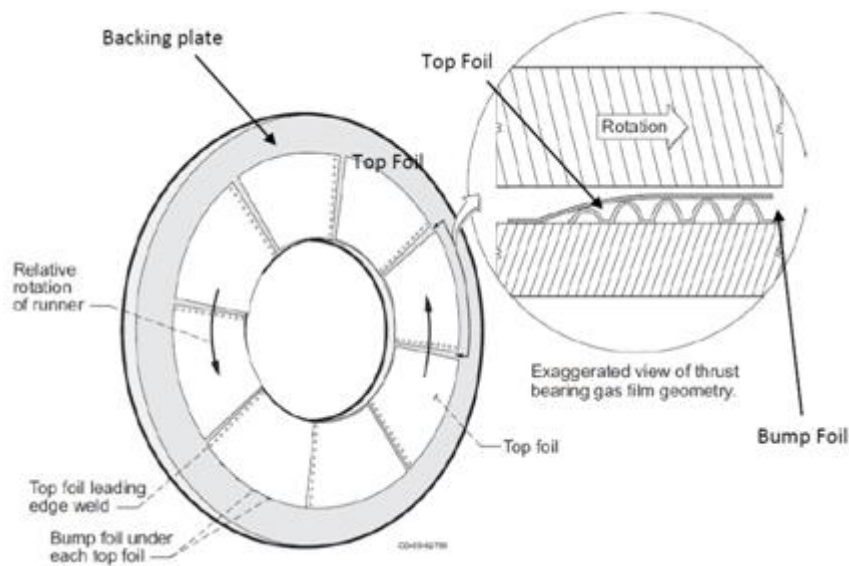


Figure 1-3 Air Foil Thrust Bearing image from [1]

### 1.3.1 Principle of Operation:

Air foil thrust bearing assembly consists of a runner and two thrust bearings, in which the runner rotates between two thrust bearings. Initially the top foils are in contact with runner. As the runner speed increases, runner drags the ambient air into the converging wedge increasing hydrodynamic pressure which results in formation of thin hydrodynamic film capable of carrying a load. To avoid friction at low speed top foils are generally coated.

Table 1-1 shows the comparison between different types of bearings. The DN number for air foil bearings is above 3 million and temperature range is from cryogenic to 1200 F, which implies foil bearings can operate at high and low temperature range, and also at high operating speeds.

Table 1-1 Comparison between different types of bearings

	Air foil bearings	Oil lubricated bearings	Rolling bearings	Magnetic bearings
DN Number	Above 3 million	Nearly 1 million	1-2 million	Above 3 million
Operating Temperatures	Cryogenic to 1200 F	90 to 180 F	-20 to 450 F	-300 to 1000 F
Oil free?	Yes	No	No	Yes although backup bearings could be grease lubricated

Applications of foil bearings include auxiliary power unit, air cycle machines, turbo alternator, Microturbomachinery, and fuel cells.

### 1.4 Motivation for studying Air foil thrust bearings.

There is a comparative dearth of knowledge on foil thrust bearings when compared to foil journal bearings. However, over the past few years work has begun for better



understanding of thrust bearings. Journal bearings typically carry the dead weight load of the shaft and the radial vibrational loads. Often there is a large axial load which is far more than dead weight of shaft. Generally to accommodate large axial loads, designers increase the size of thrust bearings. However larger diameter presents rotor dynamics problems in high speed thrust bearings.

Scope of this research is to develop an air foil thrust bearing test rig which will be capable of evaluating various parameters like load capacity, axial load, torque, temperature and pressure.

## Chapter 2

### Literature Review

Foil gas thrust bearings are self-acting, compliant-surface hydrodynamic bearings which operate on a thin lubricating gas film. To avoid rubbing contact during normal operating conditions, solid lubricants are applied to both top foils and thrust runner to prevent wear and galling during startup, shutdown and overload conditions when sliding contact occurs. Failure in the bearing is due to break down in the gas film separating the rotating component from non rotating component. Due to breakdown in the gas film or incomplete formation of gas film during startup's, shut down and normal operating conditions causes a bearing thermal runaway. Thermal runaway is due to small portion of bearing rubs with the runner causing local thermal expansion. Heshmat et al [2] were first to present the hydrodynamic analysis of foil bearings. They coupled the Reynolds equation with structural model of foils to consider compliant bump foil structure in the static performance of foil thrust bearing. Here are the few contributions made to improve the performance of air foil thrust bearing.

#### 2.1 Factors influencing the performance of foil gas thrust bearing.

This section summarize work by [3]

Dykas,B studied the effect of non ideal surface condition on the load capacity of foil thrust bearing. Measurements of bearing power loss and load capacity made in a variety of configurations highlight several important factors which influence performance. Surface condition of the top foils and surface condition of runner plays a large role in bearing performance. Thermal management is a key issue in bearing performance. Active thermal management via cooling air flow and passive thermal management via conduction through the runner have a large influence. At higher loads thermal effects are seen to be more pronounced where gas film heat generation and resulting thermo elastic

distortion are larger. To achieve high loads smooth lubricious surfaces are required, with non optimal surface conditions it is shown that asperity contacts dominates over thermal deformation.

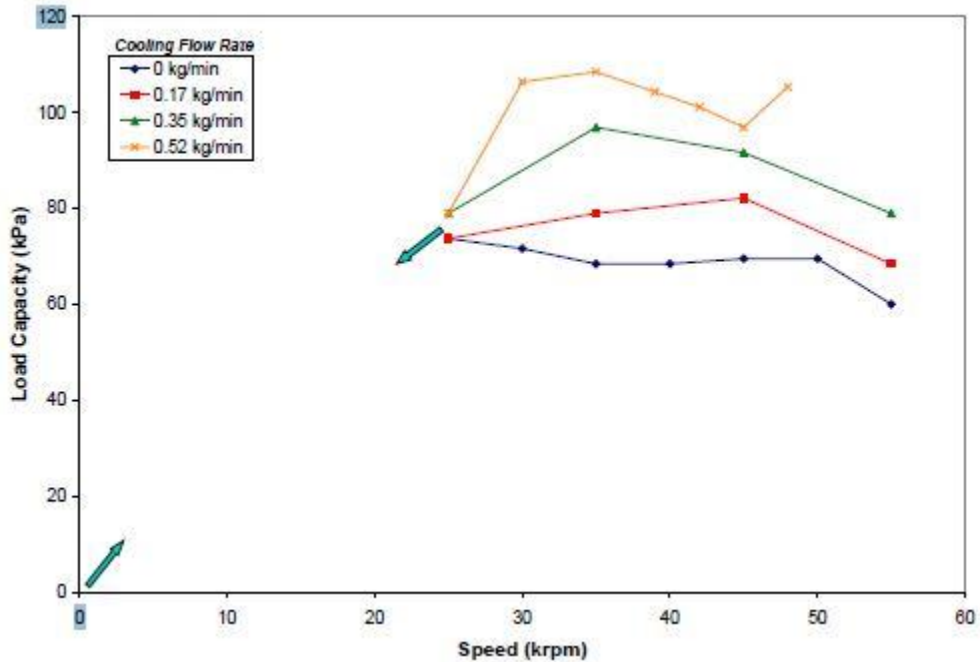


Figure 2-1 Effect of cooling air flow on load capacity, image from [3]

Dykas,B conducted various experiments to calculate load capacity against speed with varying amounts of cooling air flow through the bearings. From Figure 2-1, it is seen till 25krpm or less load capacity is insensitive of cooling air flow, but as the speed increases load capacity increases with the increase in air flow cooling. Therefore, thermal management is a key factor to achieve highest possible performance.

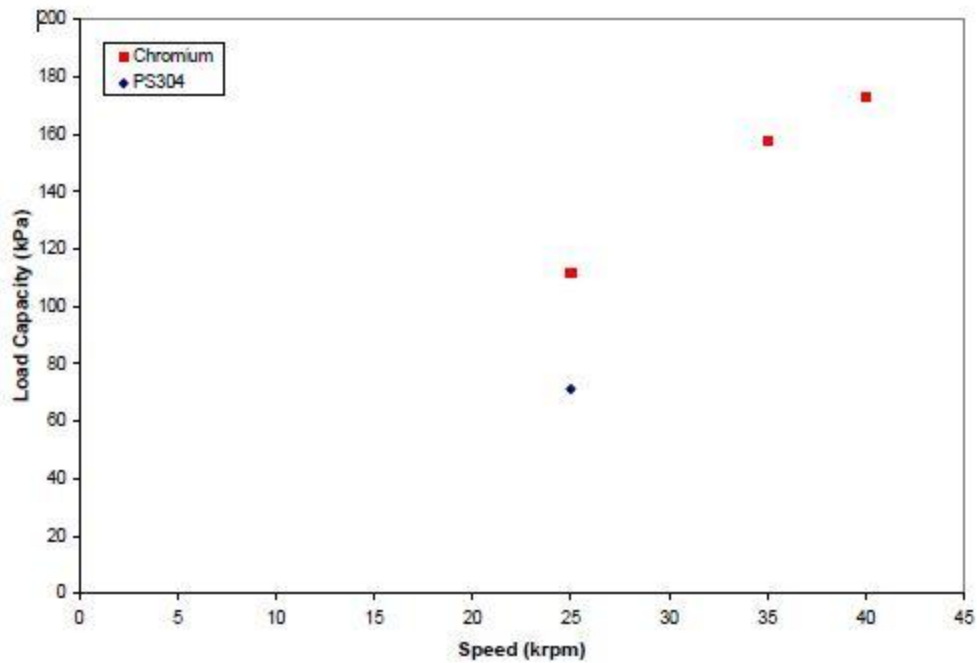


Figure 2-2 Effect of surface roughness on load capacity, image from [3]

In other experiments surface finishing effects were seen on load capacity of the bearing, using two different coatings that is thin dense chromium (TDC) and plasma spray 304 (PS304) out of which TDC being the smooth surface. By comparing the test results from Figure 2-2, it can be observed that PS304 coatings have higher load capacity than TDC. Therefore it was observed that better the surface finish, higher is the bearing performance.

## 2.2 Performance prediction of hybrid air foil thrust bearings

This section summarizes work by [4]

Air foil thrust bearings (AFTBs) has many novel features but when it comes to application of these bearings to turbo machinery with large thrust load poses significant challenges due to limited load capacity. One of the typical failures with AFTBs is severe dry rubbing

during shut down rather than start up because of large rotational kinetic energy of the rotor. To overcome this problem Hybrid Air Foil Thrust Bearing (HAFTB) was introduced.

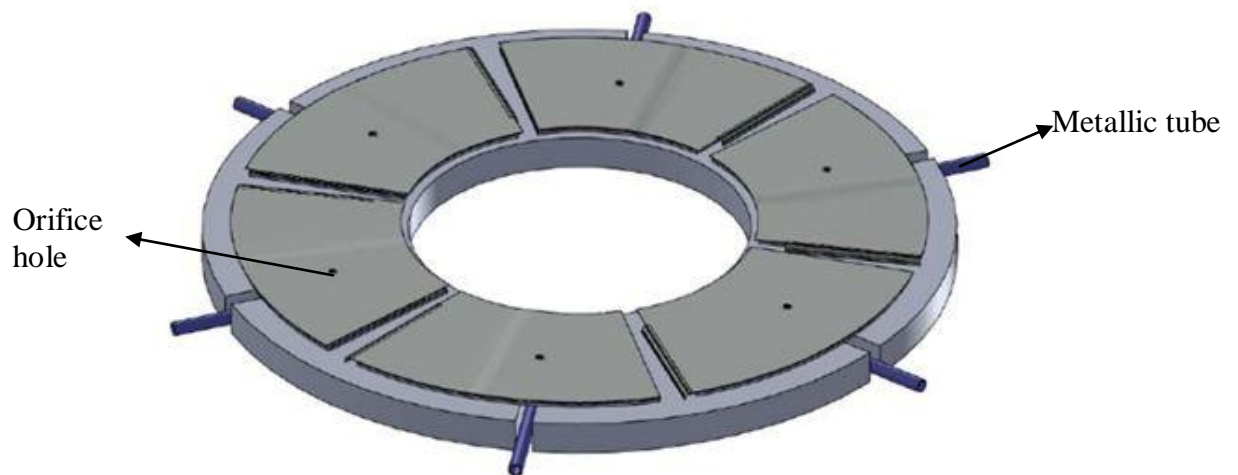


Figure 2-3 Hybrid Air foil thrust bearing, image from [4]

The study showed HAFTB has higher load capacity, much smaller torque and good cooling in comparison to the hydrodynamic bearing with traditional cooling method. Pressurized air is supplied externally through thin walled metallic tube which is laser welded on back side of the top foils. The bump foils made in this paper has several novel features such as lower manufacturing cost, prediction of bump stiffness is easier, the softer bumps at the outer edge accommodates thrust disk wobbling motion.

The pressurized air through the metallic feed tube is directly discharged through the small orifice holes drilled on the top foil. The result indicates orifice location is significant factor to increase the bearing performance, at very low speeds orifice location at the center shows best static performance. However for the entire speed range the orifice near the recess shows the best performance. It was also noticed that HAFTBs have certain film

thickness even at zero running speeds and much larger film thickness at low speeds because of which wear problem during start/stop can be reduced.

### 2.3 Gas foil thrust bearing performance and its influencing factors

This section summarizes work by [5]

Conditioning tests are run to get the bearings to maximum performance and to help them mate better with the runner. A combination of stiffness, coast down, steady state and load capacity tests give data both on the progress of the conditioning and the overall performance of the bearing. A series of start stop cycles were run to condition foil thrust bearing, which was believed to condition both the runner coating and bearing top foils from rubbing during start up and shut down. The test rig is designed to run from zero to 21Krpm, from room temperature to 1000F temperature range and the load to the bearing is 100lb. The rig is vertical mount, so the bearing is above the runner and a pneumatic loading device from above. The rig also has water and air cooling to control the temperature of the rig. The rig is equipped with thermocouples, load cell and an optical probe to provide temperature, load, torque, and speed relevant data to the test being run.



Figure 2-4 Thrust bearing configuration.

Three bearings designated as BNB001, BNB003 and BNB004 with identical bump foil configurations were run against two separate runners. Runner 1 was run against different bump foil configuration for 3000 start-stop cycles. Runner 2 was run against bearing with an identical bump foil configuration for 100 start-stop cycles. BNB001 is run against Runner 1, BNB003 and BNB004 were against Runner 2. BNB003 had a max load capacity of 75lb and BNB004 had a max load capacity of 60lb at 21KRPM after being conditioned at high temperatures and room temperatures. After being fully conditioned, BNB003 load capacity varied from 68-75lb and BNB004 varied from 50-60lb. Tests were run after the runner was removed and run on the different rig before installing it to the original rig, which shows that bearings once matched to the runner can be reinstalled and run against the runner with high degree of confidence. Runner 1 was conditioned with a bearing with different foil configuration; BNB001 achieved a load capacity of 40lb at

21KRPM. This shows a bearing operates best on a runner conditioned by a theoretically identical bearing. This allows the runner surface to be conditioned the best to interface with the top foils on that bearing design. Bearings made using same identical parts and same heat process show the repeatability of load capacity on the same runner of 30%. The difference in load capacity is due to small difference in the roughness of the bearing top foils. A single bearing run on two separate runners has repeatability in load capacity of 25%, especially if the runners have been conditioned by bearings with different compliant structure. If the runners were conditioned by same bearing compliant structure, the repeatability might be better.

#### 2.4 High Performance Foil Thrust Bearing Test Rig Developed

This section summarize work by [6]

While journal bearings have been advanced significantly, very little theoretical or experimental development work has been conducted on foil thrust bearings. As a result, to meet the increasing performance demand MiTi developed a high performance thrust bearing test rig.





Figure 2-5 Foil Thrust Bearing Rig, image from [6]

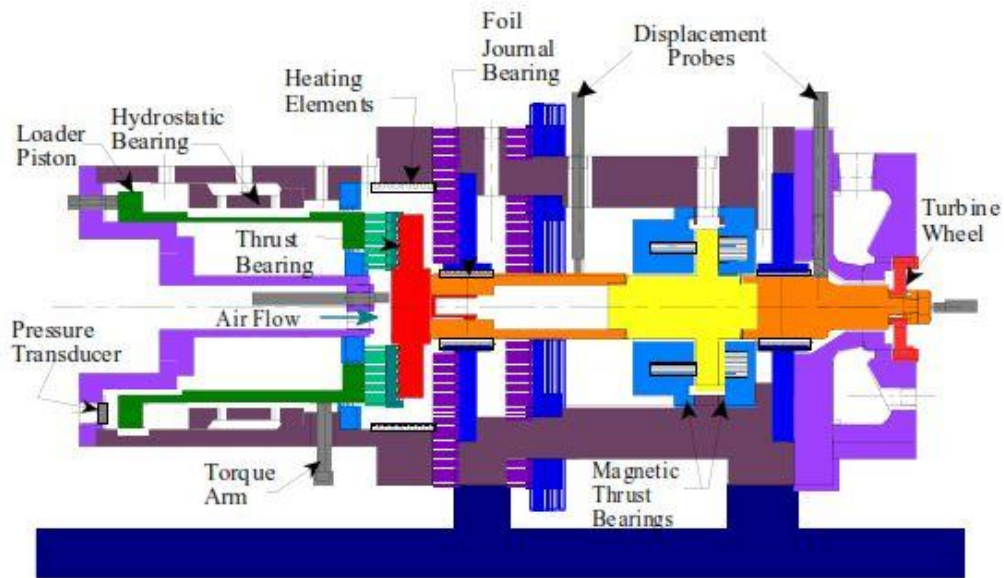


Figure 2-6 Solid Model of Thrust Bearing Rig, image from [6]

Figure Figure 2-5 figure Figure 2-6 shows a high performance foil thrust bearing test rig. The test rig is oil free using foil journal bearings as it eliminates the needs of water

cooling jacket and heat dams, foil journal bearings have DN number of over 3 million which helps the system to operate at high speed and temperature. The rig consists of a rotor which is driven by a 10 horsepower air turbine. The rotor is supported by 2 journal bearings and a magnetic thrust bearing. The test thrust bearing is mounted on a hydrostatically levitated piston so that frictionless axial and rotational motions are possible. Load on thrust bearing is generated by pressurizing the end of the loader piston housing opposite to the test bearing. High test chambers are obtained by using the electric band heater. The rig is designed to get various performance parameters of thrust bearing like speed, temperatures, torque, imposed load which are acquired using a labview system.

## Chapter 3

### Research Objective

There is a comparatively less information on air foil thrust bearing when compared to air foil journal bearings, very few researches are performed on air foil thrust bearing. This research is mainly focused on developing an air foil thrust bearing test rig which will help provide data on performance evaluation of air foil thrust bearing. The test rig is designed in such a way that it is capable of evaluating various parameters like load carrying capacity, steady state temperature, start/stop friction torque, temperature and pressure. The test rig has a push/pull mechanism which makes the stiffness measurement much easier. A sensor is developed to measure plenum temperature and pressure, the rig is efficient to measure all the parameters which will help to improve the performance of the air foil thrust bearing.

## Chapter 4

### Description of Test Rig

There is comparatively less information on foil thrust bearings due to challenges in design, manufacturing and assembly. So it was essential to develop a test rig capable of measuring parameters like temperature, pressure, load and torque. Chapter 4 comprises of detailed study of test rig set up, manufacturing of air foil journal and thrust bearings. The test rig has a push/pull mechanism which makes the structural stiffness of the bearing much easier. The test rig is equipped with thermocouple, pressure transducers, optical probes and load cell to provide temperature, pressure, vibration and load on the bearing. The developed test rig will help to enhance the performance of the thrust bearing by capable of performing experiments like effect of cooling air flow on load capacity of thrust bearing, steady state temperature, and structural stiffness of the bearing. The test rig assembly is divided into 3 main components which are:

- 10 KW Electric Motor.
- Bearing housing.
- Test housing.

#### 4.1 10 KW Electric Motor

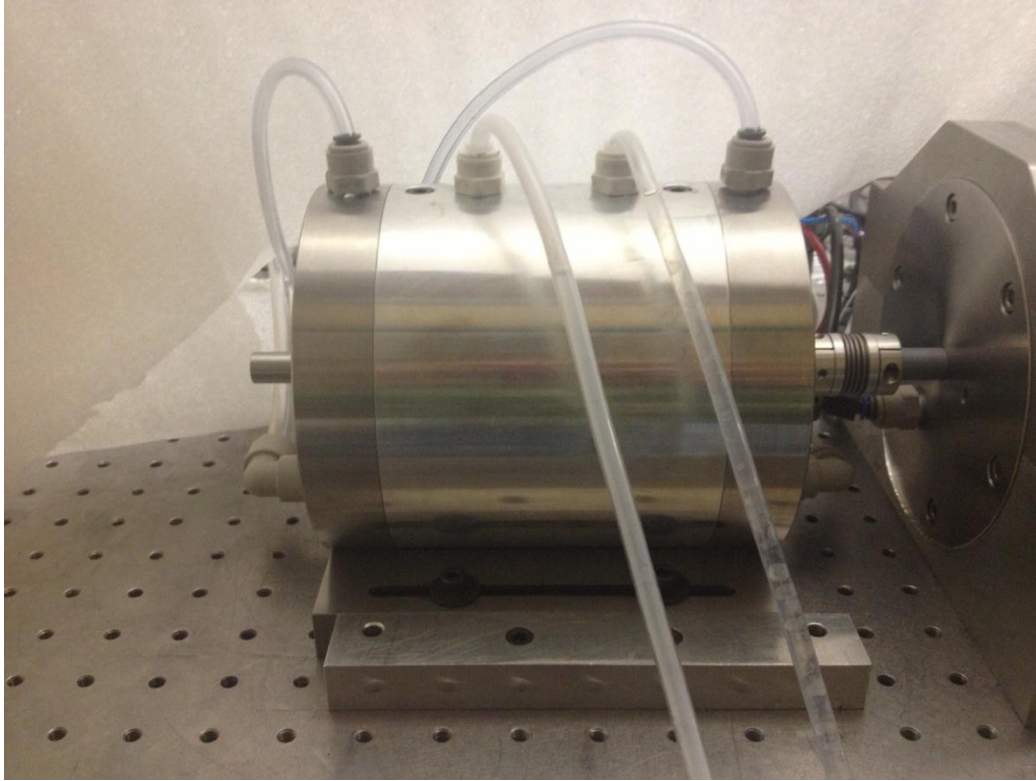


Figure 4-1 10 KW Electric motor

The motor is custom made 10KW electric motor; the parts were fabricated and machined in UT Arlington machine shop. Motor speed is regulated by frequency convertor, FC 80 series by SIEB & MEYER, Inc. Alemite 3920 oil mist lubricator is used to lubricate the bearings inside the motor. Water circulation method is used for the motor cooling. On the first test run of the motor, the failure occurred at 7,000 rpm because of the tight clearance between motor shaft and end cap. After redesigning, the end cap was made of bronze as it acts as a good lubricant. On the second test run, the motor was ran successfully up to 40,000 rpm.

## 4.2 Bearing Housing

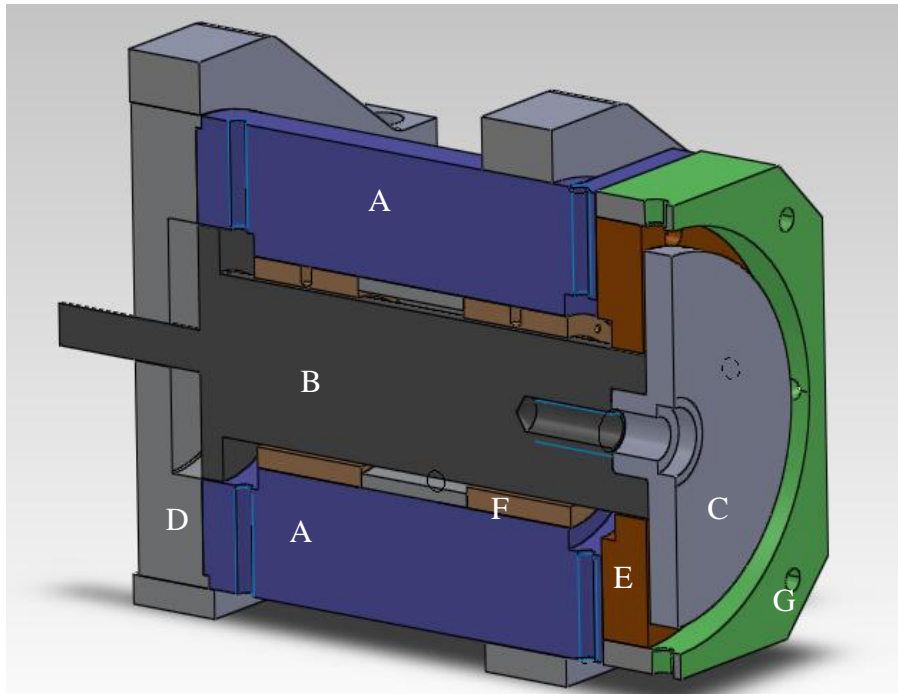


Figure 4-2 Solid Model of Cross Sectional Bearing Housing

Table 4-1 Detail Components of Bearing Housing

A	Bearing Housing
B	Shaft
C	Thrust Runner
D	Pedestal
E	Thrust Bearing Plate
F	Journal Bearing Sleeve
G	Spacer Block

Bearing housing consists of 7 components which are shaft with attached balance piston, two air foil journal bearings, thrust runner; one air foil thrust bearing and a spacer block. Housing is mounted on the pedestal. Shaft is the main part in the bearing housing as it is connected to motor through flexible coupling. Two air foil journal bearings are used to support the shaft which allows the shaft to move freely in the axial direction and also helping in dampening any minor vibrations in shaft. The two bearings are separated

by 1.5" inch spacer, which locks the bearings inside the housing. Four proximity probes are installed on to the housing to monitor vibration of the shaft. In case of any malfunction, the two journal bearings would sustain the majority of the damage before the machine could be shut down. Housing has multiple inlet and outlet holes. Two center holes on the housing are meant for cooling air flow to the two journal bearings. The balanced piston has an inlet hole which is used for applying load to the test thrust bearing. Outlet hole is to discharge air from the housing. Shaft is carefully inserted in the bearing sleeve taking care there is no damage to the bearings and top foils are in the right place. Thrust bearing back plate is mounted on to the square face of the housing on which one thrust bearing is mounted. Thrust runner is bolted on the shaft at the end opposite to the flexible coupling. Spacer block is mounted on the square face of the housing. It has three inlet ports, out of which two ports are used for cooling air flow for the thrust bearing and the third port is used to measure the temperature and pressure of the plenum.

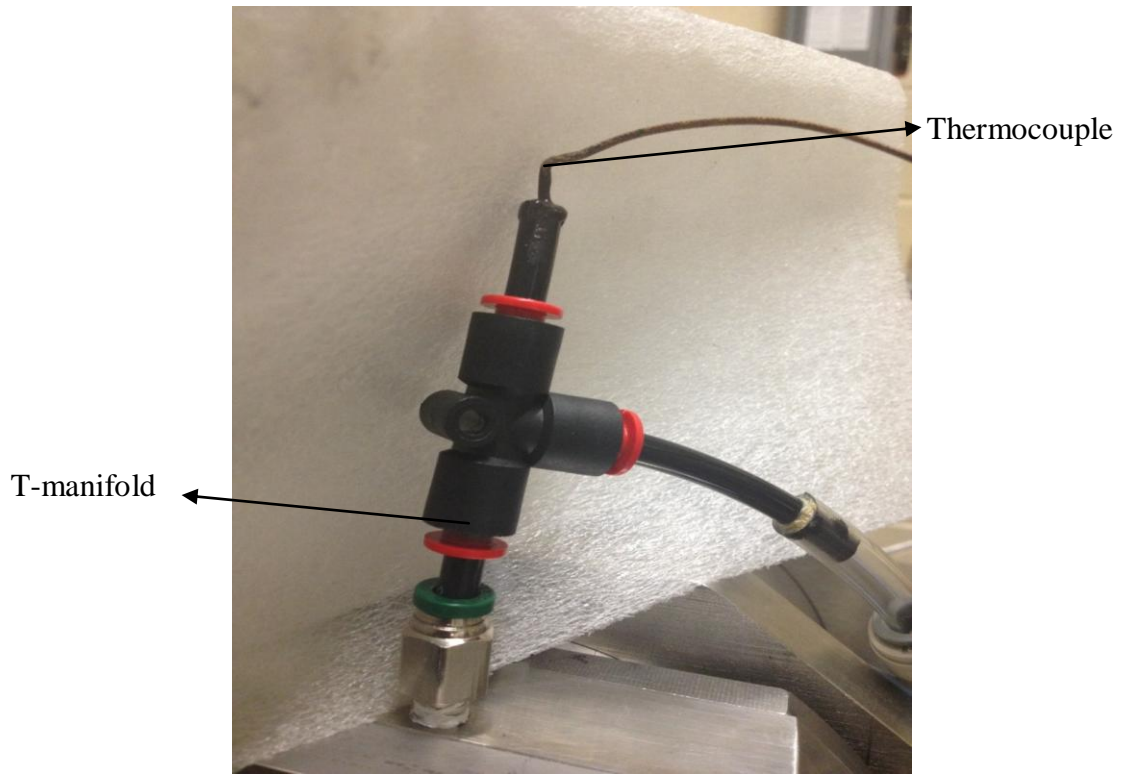


Figure 4-3 Temperature and Pressure Sensor

Temperature and pressure of the plenum is measured by using thermocouple and pressure sensor. Using a T manifold, thermocouple is fixed at the one end with epoxy, while pressure sensor is connected to one inlet and using tube the third end of T-manifold is connected to spacer to measure temperature and pressure of the plenum.

#### 4.3 Manufacturing of journal bearing

Air foil journal bearing consists of four parts which are bearing sleeve, bottom foil, bump foil and top foil. Bump foil is made of Inconel X750 0.005 inches in thickness.



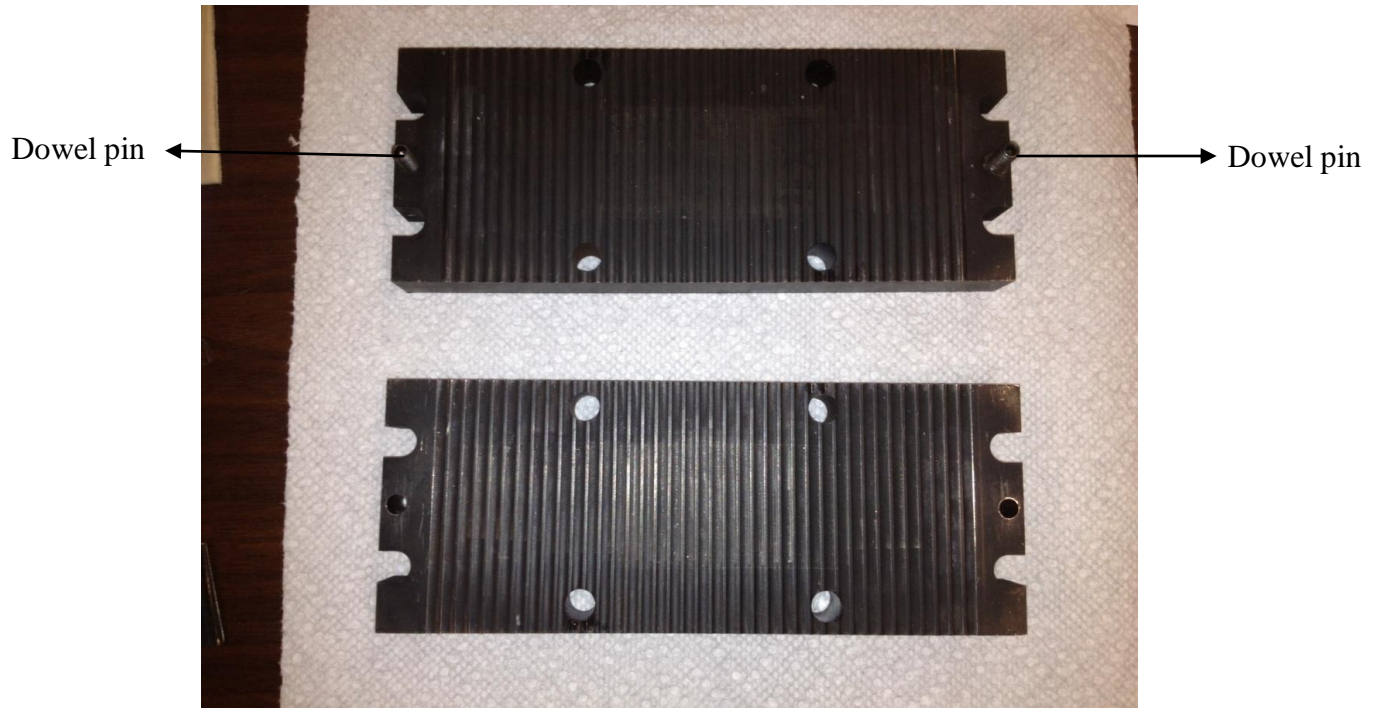


Figure 4-4 Bump foil forming jig

Bump foil is made using flat forming jig which has bumps. The bump foil blank is placed between the jig and it is pressed using a hydraulic press at 10 tons of pressure. The jig has dowel pins at both the ends, to avoid any misalignment of the blank once it is been placed on the bottom surface. Care should be taken that the bump foil blank is in the right place before placing the upper surface of the jig.

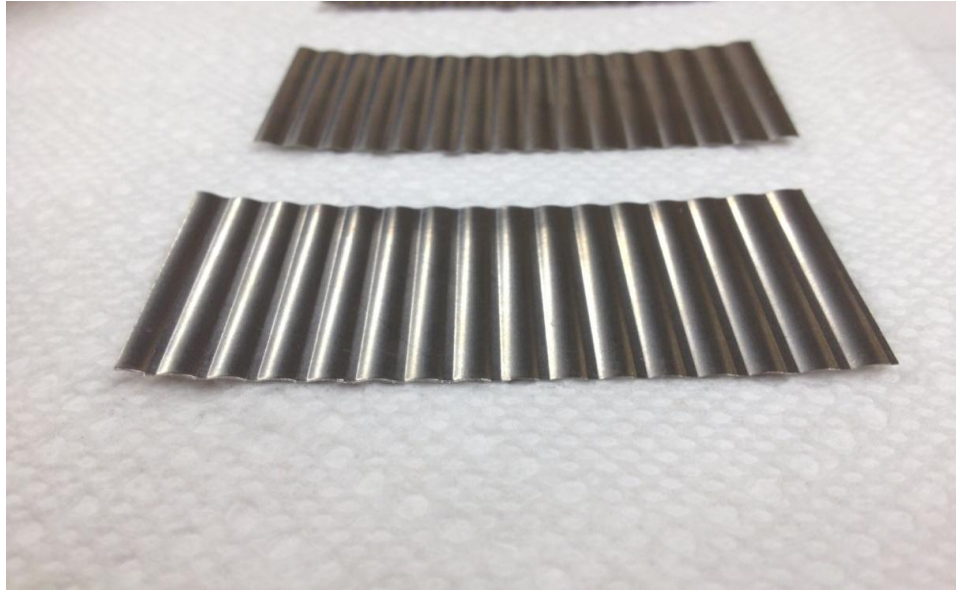


Figure 4-5 Bump foils after hydraulic press

This is how bump foils look after hydraulic press. Next step is to heat treat the bump foils in an automated electric furnace for 18 hours. Before heat treatment, the bump foils is given a curvature like bottom foils so that it has smooth curvature. Flat bump foils are placed over the bottom foil, and then it was pressed against the shaft uniformly giving the bump foil a smooth curvature like the bottom foil. After heat treatment, bump foil are spot welded over the bottom foil. Top foils are coated with Teflon to avoid friction at low speeds.

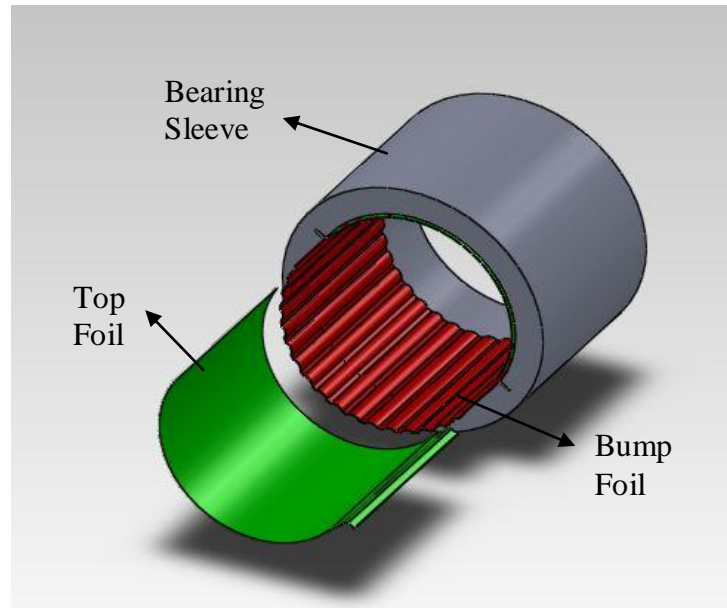


Figure 4-6 Assembly of journal bearing

The bearing sleeve has a groove meant for top foil and bottom foil. Depending upon on the direction of rotation the top foil and bottom foil are placed in the groove. The direction in journal bearing is from free end to fixed end.

#### 4.4 Manufacturing of thrust bearing

Air foil thrust bearing consists of three components which are base plate, bump foil and top foil. Two air foil thrust bearings of different kind were made, one with Rayleigh step contour top foil (Bearing A) and other one is taper contour top foil (Bearing B). Bearing A consists of four components which are base plate, bottom foils, bump foils and top foils. Base plate is made of 0.008 inch thickness of stainless steel, which is made by wire Electrical discharge machining (EDM) process.



Figure 4-7 Base plate for thrust bearing

The next step in the assembly is to make bump foils. Bump foils are made from nickel chromium alloy called Inconel X750. Inconel X750 are very ductile and easily formable prior to heat treatment. Inconel X750 sheets of 0.005 inch thickness is used to make bump foils.

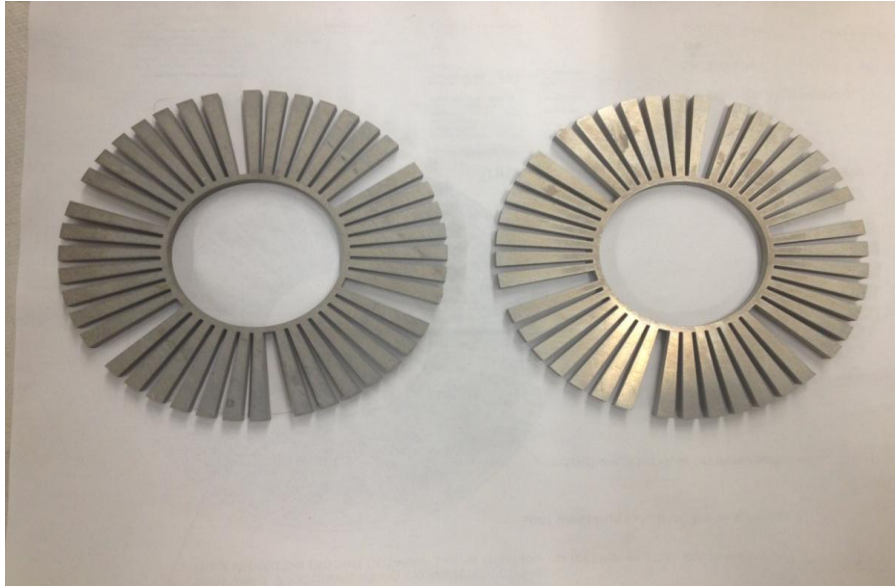


Figure 4-8 Bump foil Blanks

Blanks of the bump foils were made using wire EDM process.



Figure 4-9 Bump foil forming jig

The design allows lower manufacturing cost as the jig used in the formation of bump foils can be made using a precision lathe. The bumps are connected to inner frame of the base plate hence the assembly of the bump foils and base plate can be self aligned and requires minimal spot welding [8]. As each foil strips moves along the radial direction, prediction of bump stiffness is much easier. By changing radial pitch, height and width of the slots it is easy to control stiffness distribution along radial and circumferential directions. Thrust disk's wobbling motion is a most frequent failure mechanism which occurs in thrust bearings. This failure can be minimized by using same radial pitch and height which results in softer bumps towards outer edge [8]. After the blanks were ready, using a manual hydraulic press and applying approximately 10 tons of pressure bump

foils were made. After hydraulic press the bumps were heat treated in an automated furnace for about 18 hours.

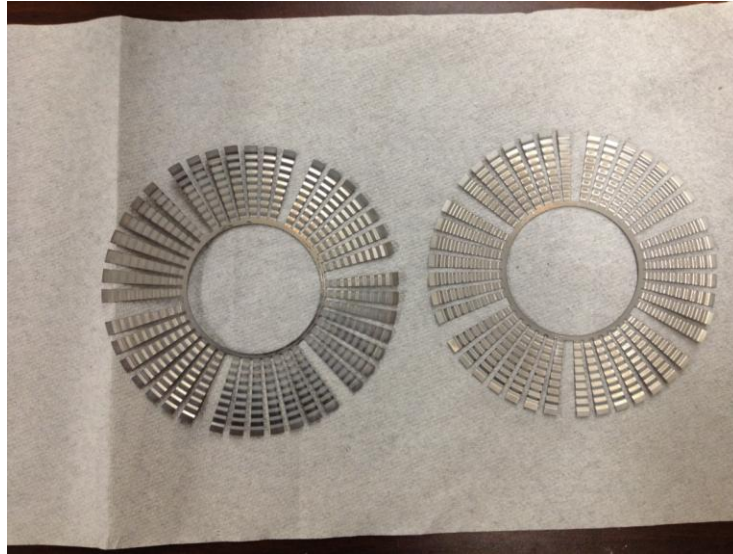


Figure 4-10 Bump foils

Novel features of bump foil structure:

The elastic foundation made is patent pending which was designed by Kim [8], which has several novel features when compared with other bump foil structure. The radially arranged bump foils are connected to the inner frame so that the bump foils can be easily aligned to inner radius of the thrust plate during assembly.





Figure 4-11 Prototype bearing with one top foil removed image from [1]

If cooling air is introduced to these bump foils, the flow is not radial. Recent commercial AFTB's may have different bump foils arrangements, which might be even more complicated. Using this type of flow channel makes the prediction of thermo dynamic very difficult and thermal management very challenging in terms of supply pressure control and cooling air flow distribution.



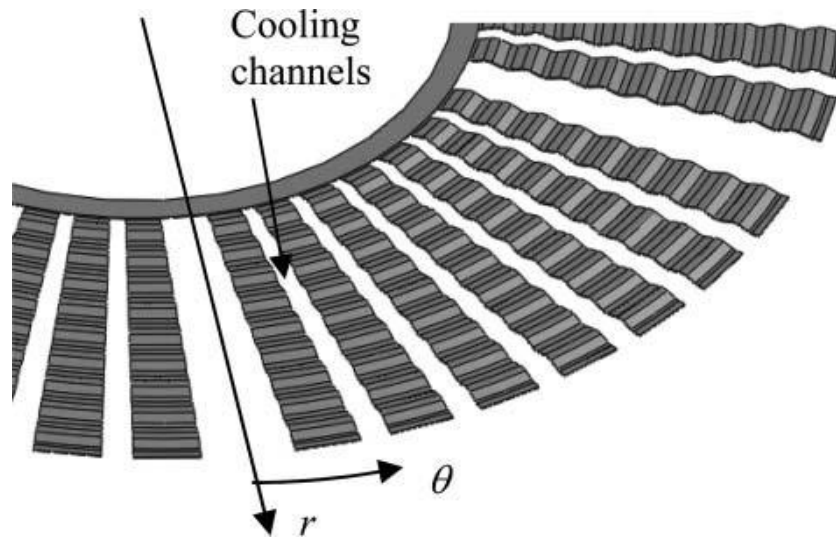


Figure 4-12 Radially arranged Bump foils image from [8]

Radially arranged bump foils makes the prediction of bump stiffness much easier due to the radial motion of each foil strip. Using the same radial pitch and height results in softer bump support towards the outer edge, softer bump at the outer edge accommodates the thrust disk runner's misalignment, which is one of the frequent failure modes of thrust bearings [8].

Next step is to make top foils. Top foils are made of Inconel X750 which requires more precision than bump foils. The top foils components must be made in a mirror form, this mirror form is facilitated by using mirror forming jig as shown in Figure 4-13, which allows two mirror images top foils pieces to be made simultaneously. The blanks are placed in a hydraulic press and 10 tons of pressure is applied on each side. A 0.002 inch step is formed from the centre of the foil till the free end. The step is designed to create a pressure difference circumferentially across the face of the bearing. A sharp cornered piece of steel is used along with hydraulic press to form a sharp step down on one side of a foil.



Figure 4-13 Top foil jig

The bottom foils were made using a dimensional drawing in a physics machine shop using wire EDM. The bottom foil has the shape similar to top foils it used to raise the height of the bump foil from the base plate by 0.002 inch.



Figure 4-14 Rayleigh Step top foil

To minimize the wear during start/stop cycles and low rpm, top foils are coated by Teflon.

Below are the all components needed to make a Bearing A.



Figure 4-15 All the parts to assemble thrust bearing

To assemble thrust bearing, bumps foils are spot welded on the base plate using a spot welding machine. Special care should be taken while performing spot welding. Applying excess of weld energy might damage the bearing. Hence, using an appropriate weld energy bump foil was welded on the base plate. After which bottom foil was slid between the base plate and bump foils to raise the height of bump foil by 0.002 inch. The bottom foils were welded between the arms of the bump foils. Depending upon the direction of the thrust runner top foils are welded accordingly, direction in thrust bearing is from fixed end to free end. Below is the Figure 4-16 of Rayleigh step bearing.

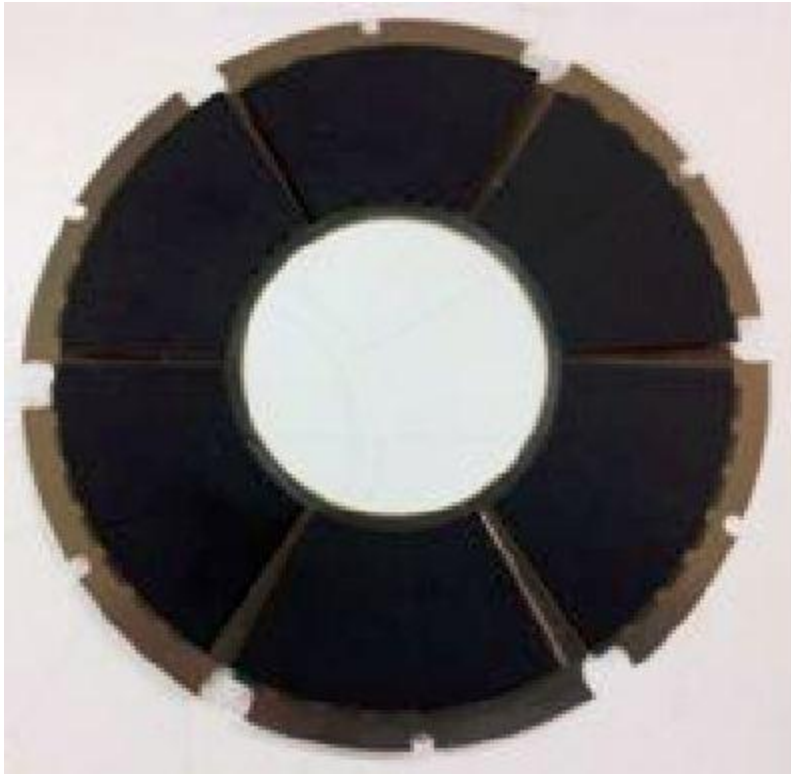


Figure 4-16 Rayleigh Step Bearing

Bearing B consists of three components which are base plate, bump foil and top foils. Base plate is made using the same process as it was used in bearing A. Bump foils are made using the same process, after the formation of bump foils from hydraulic press two foil strips from each sector are removed which is shown in Figure 4-17.

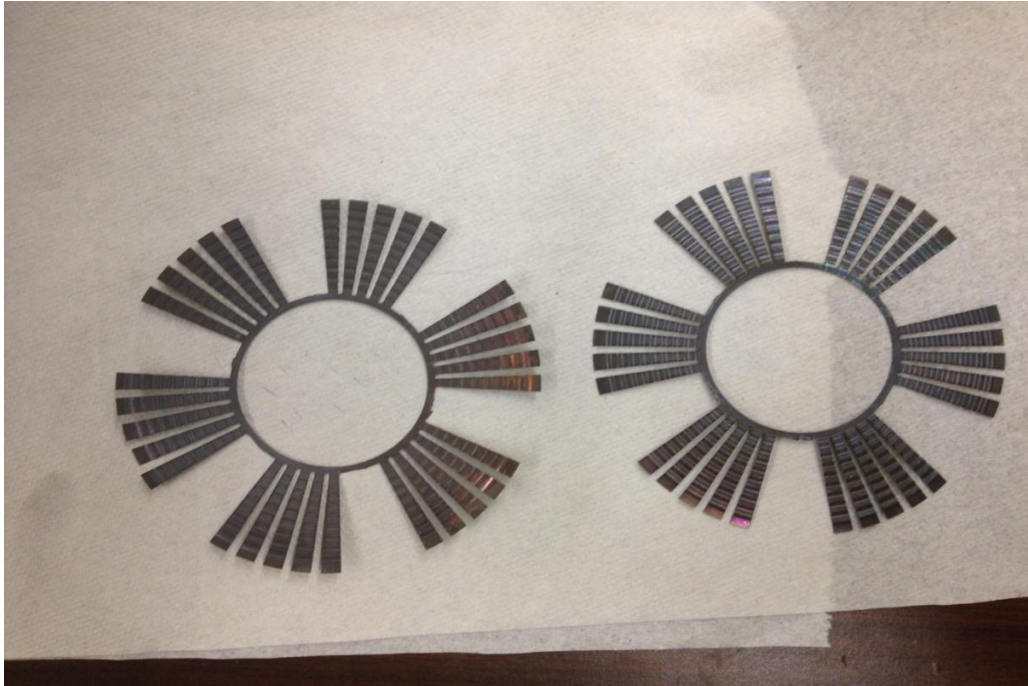


Figure 4-17 Bump foils after removal of 2 strips from each sector

After the removal of two strips from each sector, bump foils are heated treated in an automated furnace for 18 hours. The top foils in the bearing B are made of 0.005 inch thickness of stainless steel as seen in Figure 4-18. Blanks were sent to True Cut in garland using a wire EDM process top foils were made. After which top foils were sent for Teflon coating to avoid wear during start/stop cycles and low rpm.

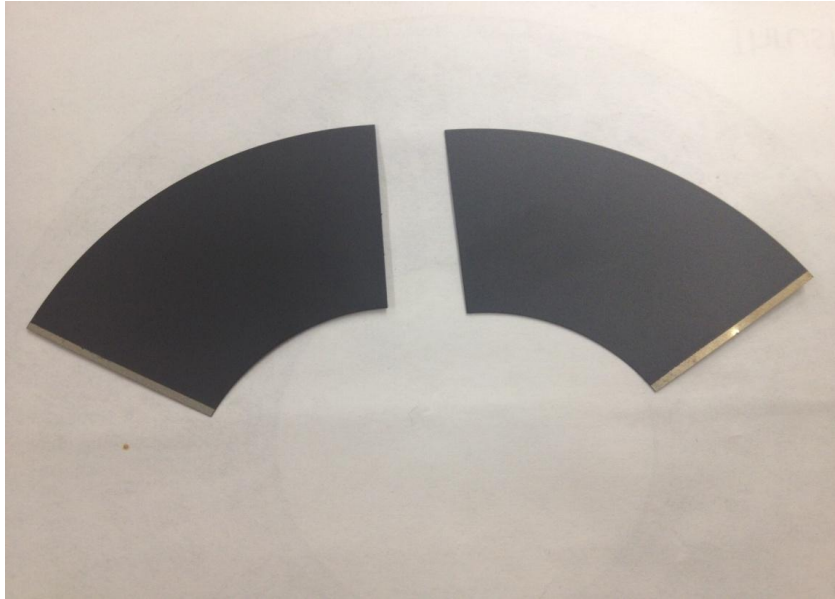


Figure 4-18 Top foil for Bearing B

Assembly of the thrust bearing is done by spot welding machine using a correct welding energy. Bump foils are welded on the base plate, inner frame of the bump foils are welded on the base plate. Depending upon the direction top foils are welded accordingly. Here is the Figure 4-19 of taper flat thrust bearing.

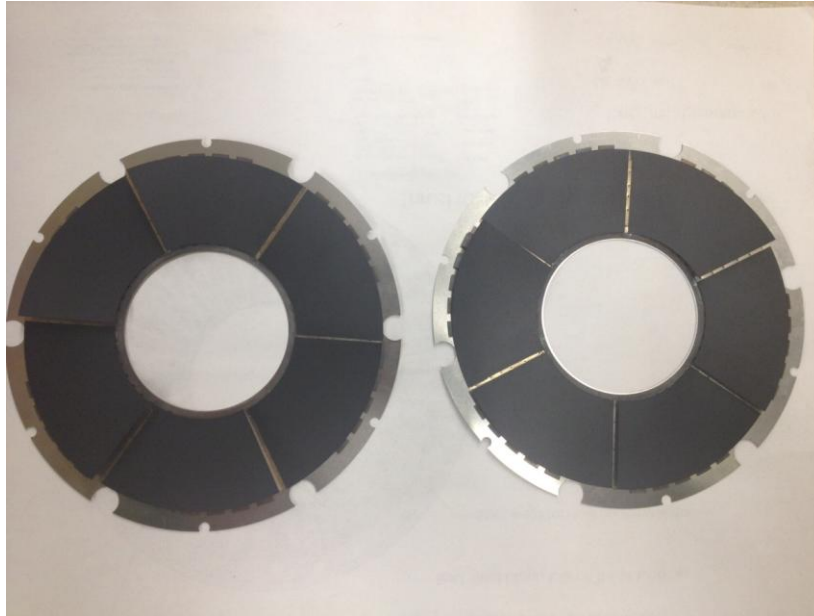


Figure 4-19 Taper flat thrust foil bearing.

Bearing is mounted on the bottom plate and bottom plate is mounted on the square face of the housing. Thrust runner is bolted on the opposite side of the flexible coupling end. All the proximity probes were installed on the housing to monitor vibration of the shaft. Next step in the assembly was to align motor shaft and housing shaft. It is very critical to align the motor shaft and housing shaft perfectly, as any misalignment will cause vibration and resulting in the structural housing damage. The centre height of both the shaft was measured using a height gauge, it was noticed that housing shaft height was less by 1 mil than motor shaft. To match the shaft height heavy duty kitchen foil of 1 mil in thickness is used as a shim. The shim was placed between the housing and pedestal. After both the shafts were aligned perfectly, a guide block was set for the motor to align perfectly all the time. Both the shafts were attached using a flexible coupling. To check whether motor and housing are completely aligned, the motor was run successfully to 40,000 rpm without any damage. Proximity probes were installed to monitor vibrations, in case of sudden increase in vibration amplitude at higher speeds.



#### 4.5 Test housing

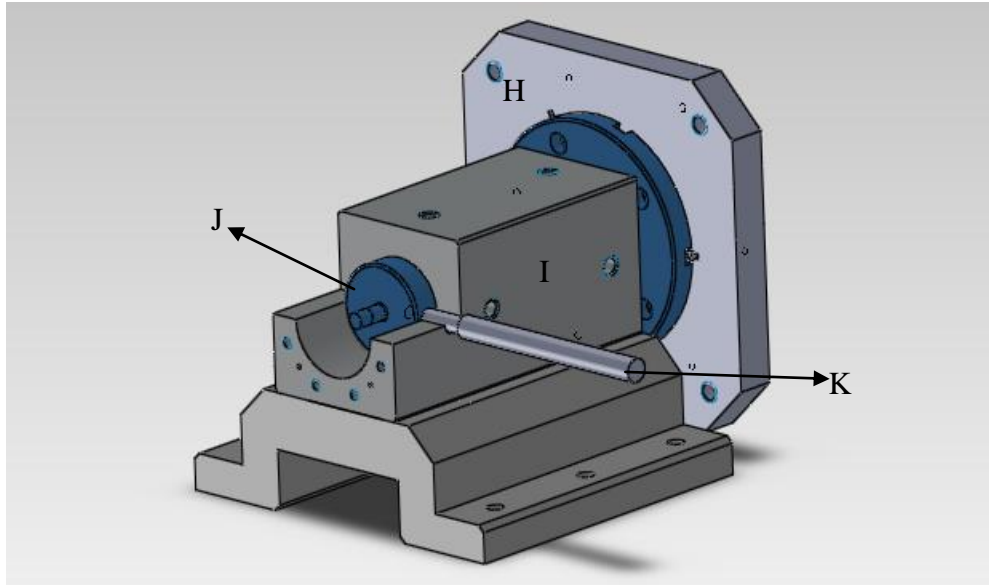


Figure 4-20 Solid Model of a Test Housing.

Table 4-2 Components of Test Housing

H	Thrust Bearing Back Plate
I	Square Housing
J	Shaft
K	Connecting Rod

The test housing was designed to be square as high precision was required for shaft height; the square housing allows easier machining and more precise tolerance. The pedestal on which housing is mounted is built with high tolerance. The housing is built with high tolerance and parallelism of bottom and top surface to avoid any misalignment of the shaft. The test housing contains all the vital components required to conduct analysis of air foil thrust bearing. 8 quarter inch air fittings were attached to the test housing so that the shaft is air borne when supply air is turned on. Components of test housing are shaft; thermocouple to monitor temperature across the bearing face, torque load sensor is designed with torque arm which is connected to the shaft. Six holes were



drilled on the backside of the back plate where thermocouple will be mounted. Attaching thermocouple to these six drilled hole was a challenging part. Firstly, super glue was used to attach the thermocouple inside the cavity. However, it was an unfruitful event as super glue attached the thermocouple on the periphery rather than at the bottom of the hole. Secondly, tried to attach thermocouple by spot welding using a small metal piece, as the holes are very small in diameter it was not possible to attach the thermocouple using spot welding. Dr.Kim suggested an idea of using a screw to attach the thermocouples; it came out to be the right approach. Thermocouple end was super glue to the head of the screw which was then super glued to the bottom of the hole; by this method all of the six thermocouples were attached to the back plate of the thrust bearing to monitor the temperature across the bearing face. Torque arm is a rod which is connected to the end of the shaft. Torque load sensor is compressed between the plates by using a loading mechanism through cable which is connected to the end of the rod.

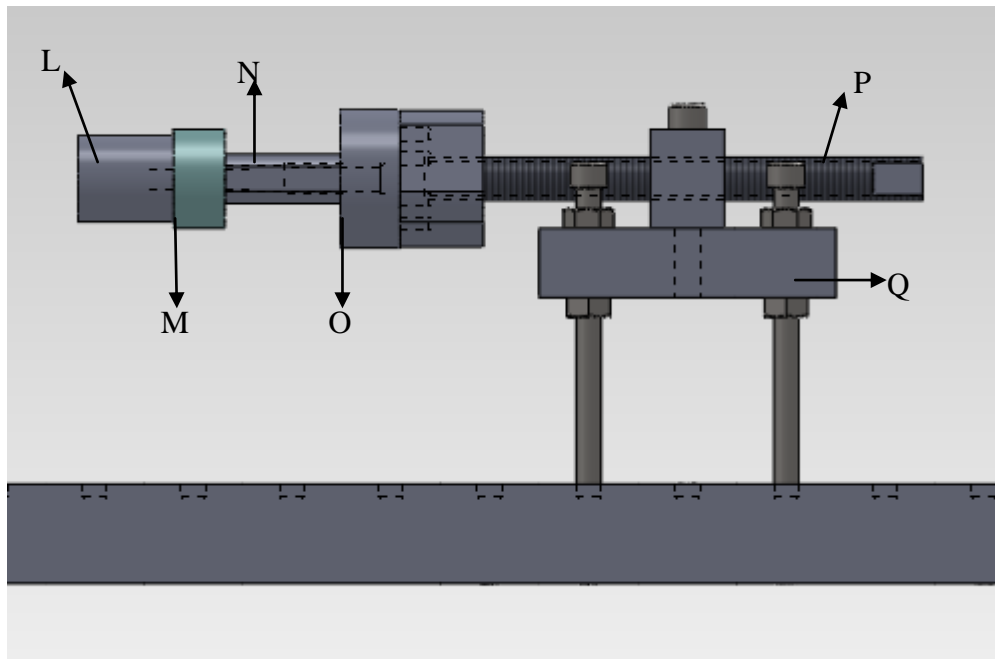


Figure 4-21 Push Pull Mechanism

Table 4-3 Detailed Components of Push Pull Mechanism

L	Bearing Adapter
M	500 lb Load Cell
N	Load Cell Adapter
O	Push Pull Mechanism
P	Screw
Q	Pedestal

The shaft that runs through the test housing is machined smaller in diameter at the end opposite to thrust bearing to accommodate bearing adapter which has a groove meant for two washers and a thrust bearing. The other end of the bearing adapter is connected to load cell, where load cell is used to measure axial load on the bearing. Load cell is connected to load cell adapter and other end of the adapter is connected to push pull mechanism, both ends of adapter have corresponding size of taps for connecting it to load cell and push pull mechanism. Push pull mechanism is a cylinder which houses the piston and a pair of thrust bearing on both sides. The piston cylinder arrangement converts rotating motion of screw into linear motion. One end of the screw is manually rotated using a wrench. Once the screw rotates with reference to fixed pedestal, along with rotary motion it either pull's/push's the cylinder. This pull/push force is transmitted to the other end of the piston through thrust bearing. Push/pull mechanism is connected to pedestal, which is a simple structural member in which screw rotates. Pedestal is mounted on metal platform supported by four fully threaded long screws. Platform is held in place by eight nuts, four on top and four on bottom of the platform, because of which the height of the platform can be adjusted depending upon the shaft diameter. Once all the parts were assembled the test rig was ready to perform experiments on.

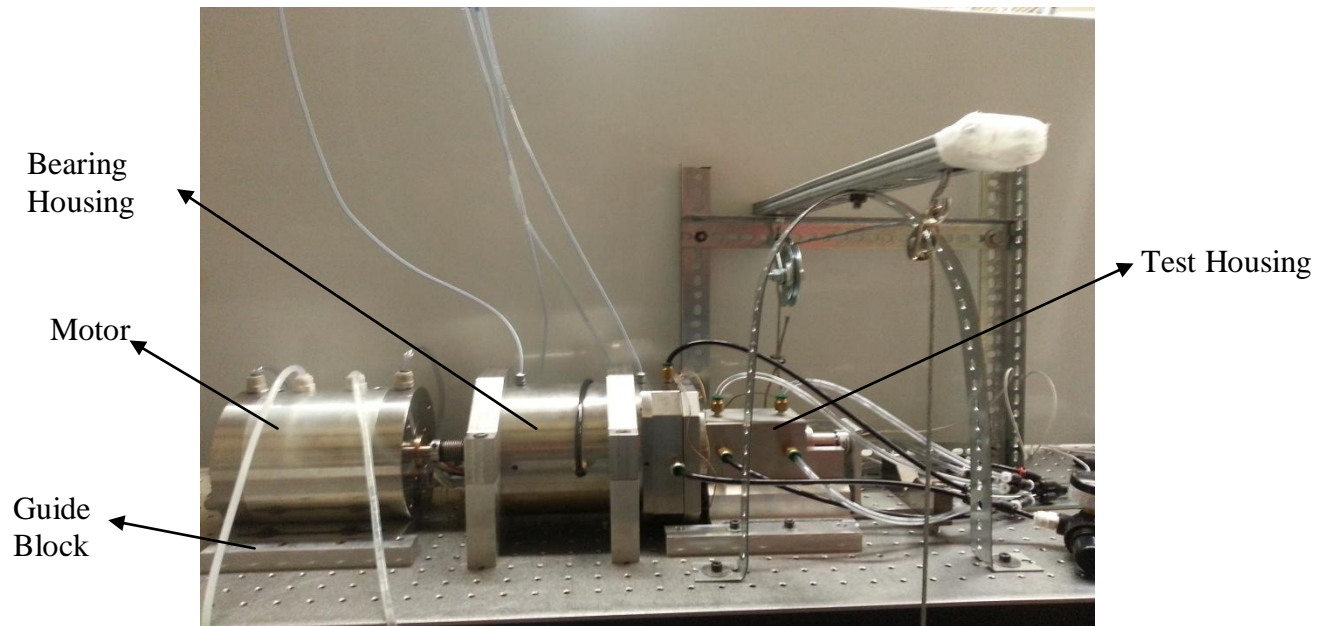


Figure 4-22 Test Rig Assembly

#### 4.6 Instrumentation

The test rig is designed in such a way that it can evaluate various parameters which will help enhance the performance of the thrust bearing. The following parameters are temperature, pressure, torque and axial load.

##### 4.6.1 Temperature Measurement

K type thermocouple is used to measure temperature across bearing face and plenum temperature. Thermal management is a key issue in bearing design hence to monitor temperature at every moment is really important. The test set up is designed such a way that on the backside of back plate of the test thrust bearing has six holes which are meant for thermocouple to measure temperature across the bearing face as shown in Figure 4-23.

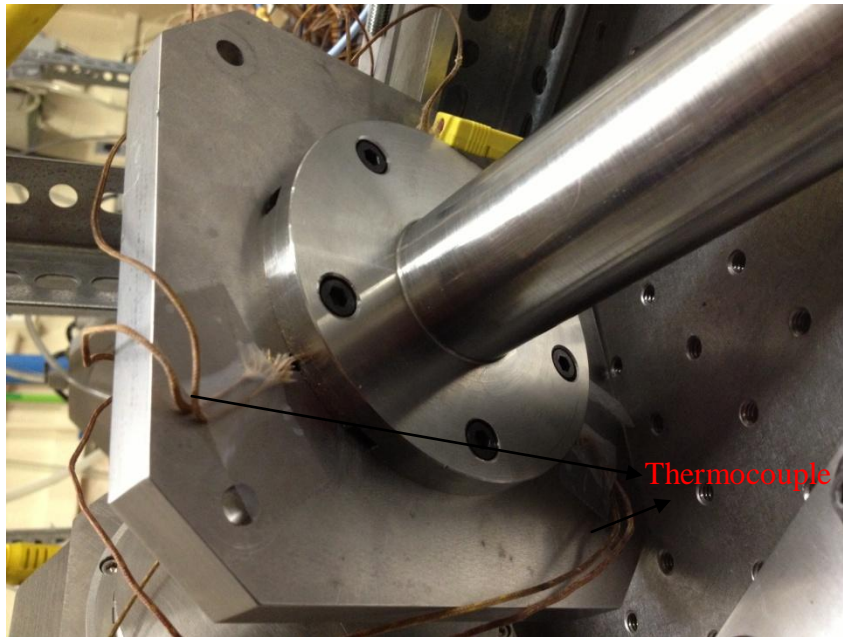


Figure 4-23 Attached Thermocouple at the Back Plate

The plenum temperature is calculated using a T manifold as shown in Figure 4-3. The temperature data is collected using a National Instrument device NI 9213. The temperature module is attached to the chassis NI cDAQ-9174 which contains the systems data, timing, triggering buses. The chassis was connected to computer via USB port and the LabView VI was built to store and display real time data.

#### 4.6.2 Pressure measurement

Pressure transducers (PX409-2.5G5V) from Omega, Inc were used to measure plenum pressure using a pressure and temperature sensor as shown is Figure 4-3 and another T- manifold is used to measure pressure at the inlet of the piston. Piston pressure is regulated by using a pressure regulator. The voltage signal from transducer was processed through the NI 9205 input module. The module is then attached to the chassis NI cDAQ-9174 and which is connected to computer via USB port. Custom built LabView VI was used to process voltage to pressure.

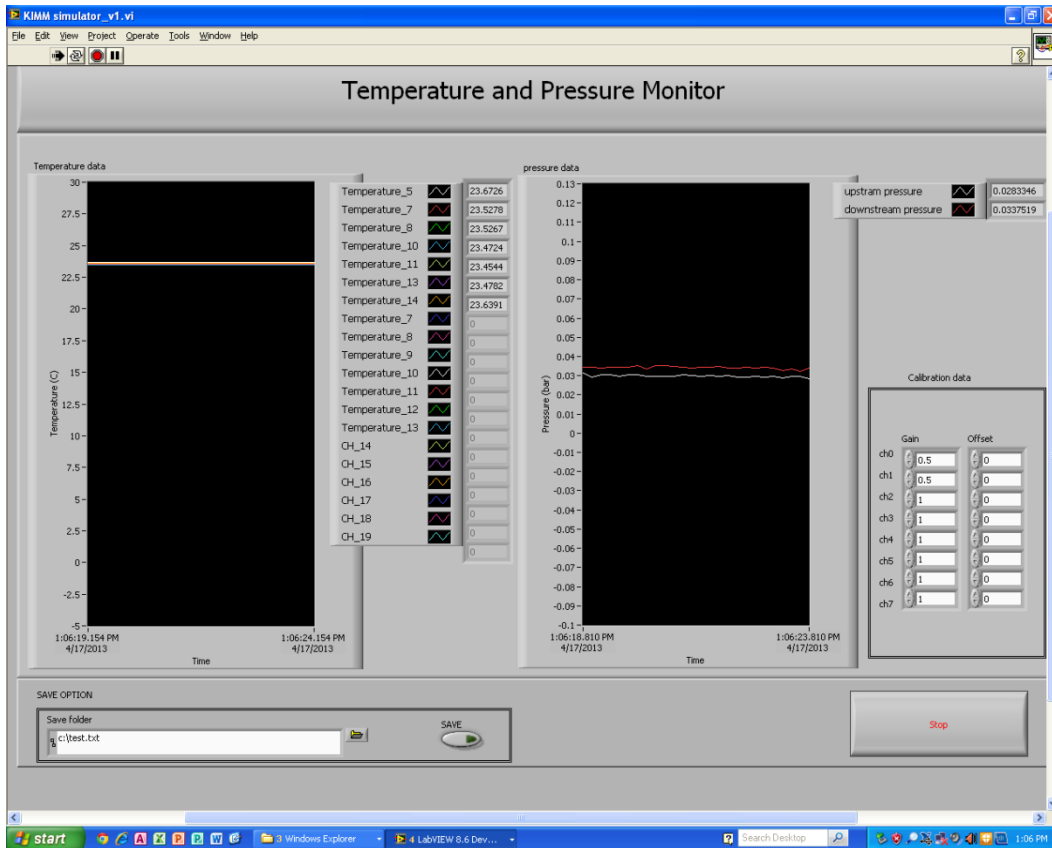


Figure 4-24 Temperature and Pressure VI

#### 4.6.3 Vibration measurement

Structural housing consists of four 3300 XL 8mm proximity transducer system. The system provides an output voltage that is directly proportional to the distance between the probe tip and the observed conductive surface. It can measure both static position and dynamic vibrations.

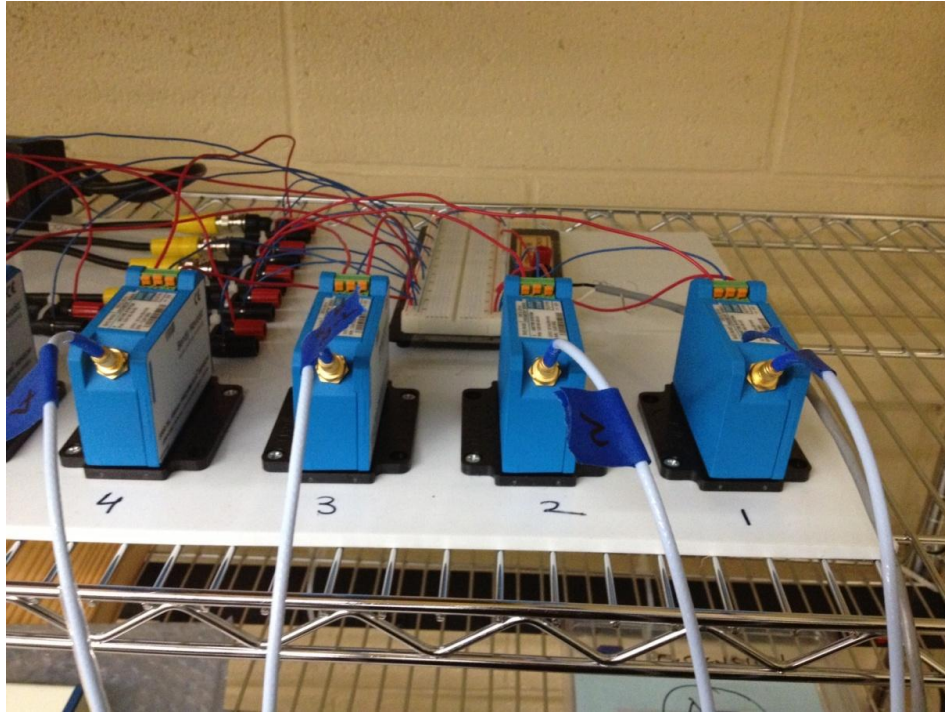


Figure 4-25 Proximity Sensor Connectors



Figure 4-26 NI USB 4432 DAQ



The probes are connected to connectors using an extension cable. These connectors are wired to breadboard with proper positive, negative and ground terminals. It is then connected to NI USB-4432 via two way cable to read voltage from the sensors. Two probes in horizontal and vertical direction are installed to monitor front and rear vibrations of the shaft. Using a custom built LabView VI to monitor and save vibrations at real time.

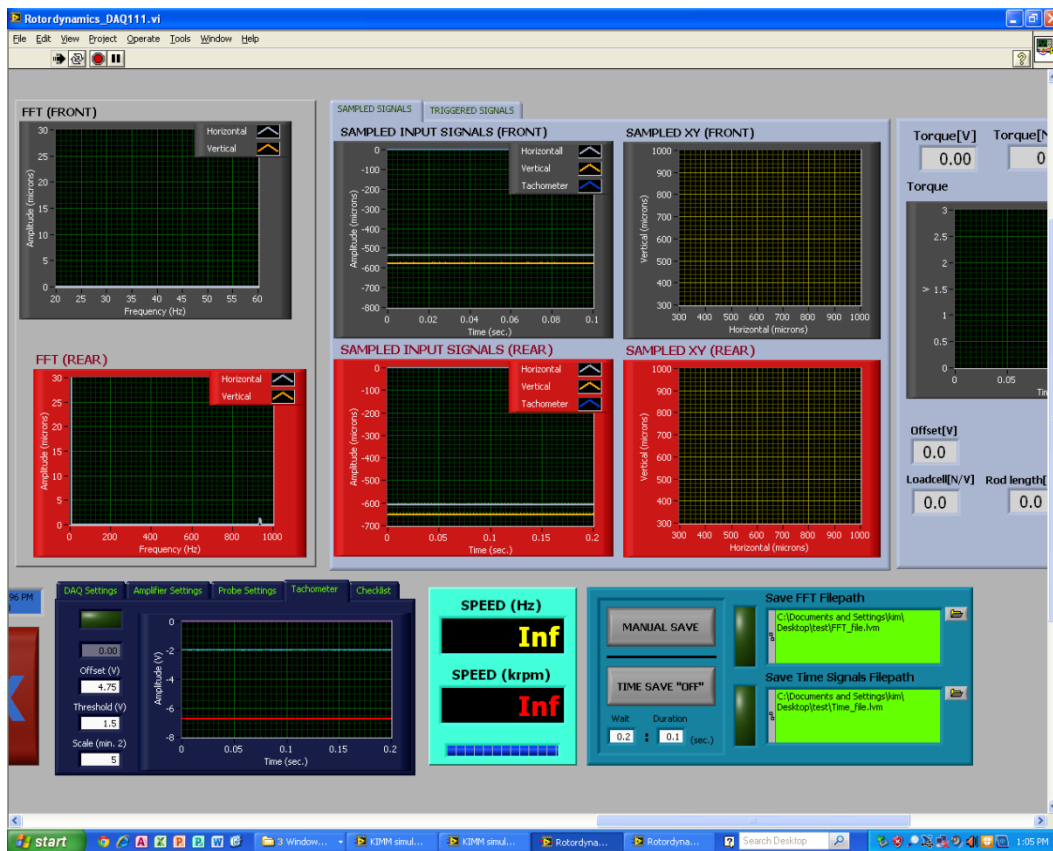


Figure 4-27 Vibration measurement VI

#### 4.6.4 *Stiffness and runner displacement measurement*

To measure runner displacement two proximity probes are installed, one at the piston end and other one at the backside of the back plate of test thrust bearing. Runner displacement is measured by subtracting displacement by the two probes from their initial point, using LabView VI to measure the displacements by two probes. Stiffness is

measured using a push pull mechanism as shown in the Figure 4-21, one proximity probe is installed at the backside of back plate, using the mechanism the screw is rotated that it push the back plate against the bearing face and displacement of the bearing is measured by proximity probe. Using a LabView VI to measure the displacement and force a graph is plotted against force and displacement giving the stiffness of the bearing.

#### 4.6.5 Torque measurement

In order to prevent sudden failure and damage to the test rig, torque monitoring is very important. A torque rod is attached at the end of the shaft as shown in Figure 4-288 where bearing friction force is transmitted to PCB 201B07 load cell via torque rod. The load cell signal is connected to low speed pressure DAQ NI 9205 channel which is then connected to computer via USB cable. Using torque measurement LabView VI, torque is measured.





Figure 4-28 Torque Rod attached to shaft

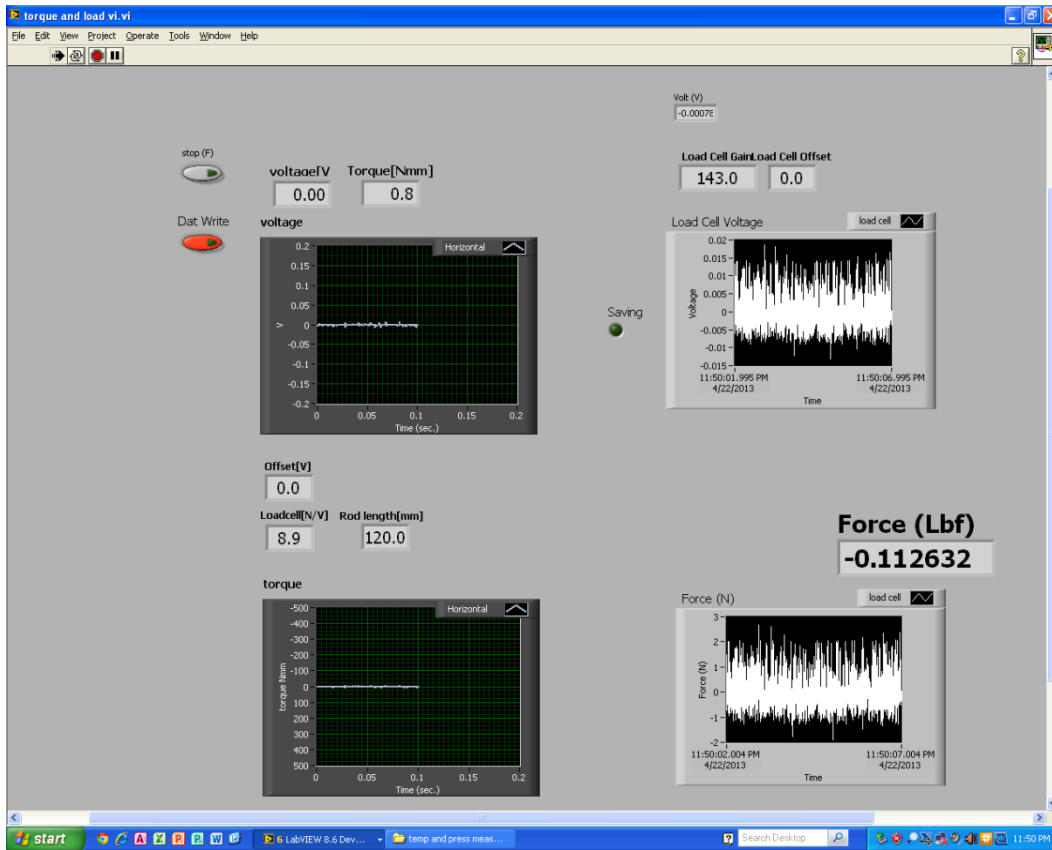


Figure 4-29 Torque and Load Measurement VI

## Chapter 5

### Results and Conclusion

#### Structural Stiffness

Structural stiffness of the Rayleigh step bearing is measured using a push pull mechanism as shown in Figure 5-1. The assembly consists of proximity probe which is calibrated against the shaft. The thrust runner is pressed against the bearing face and the applied force is measured by axial load cell which is connected to push pull mechanism. To measure stiffness of the bearing a graph is plotted force against displacement as shown in Figure 5-22 and Figure 5-3.

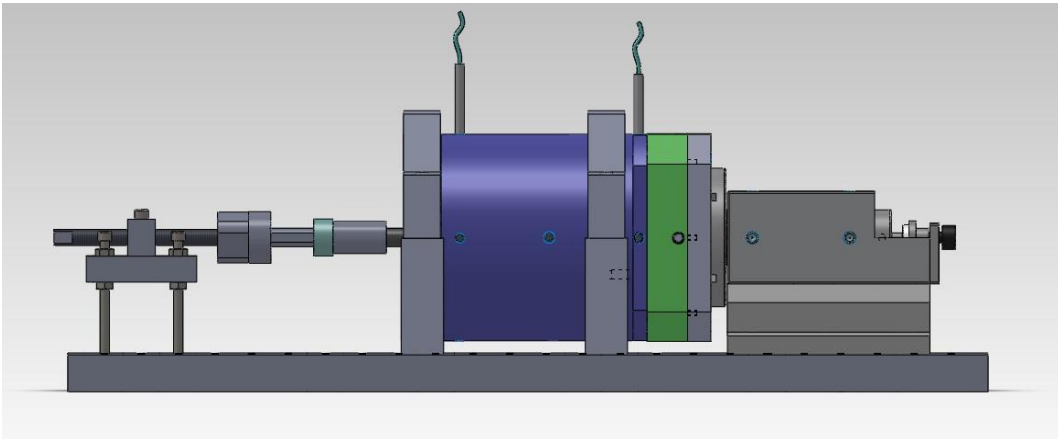


Figure 5-1 Structural Stiffness assembly

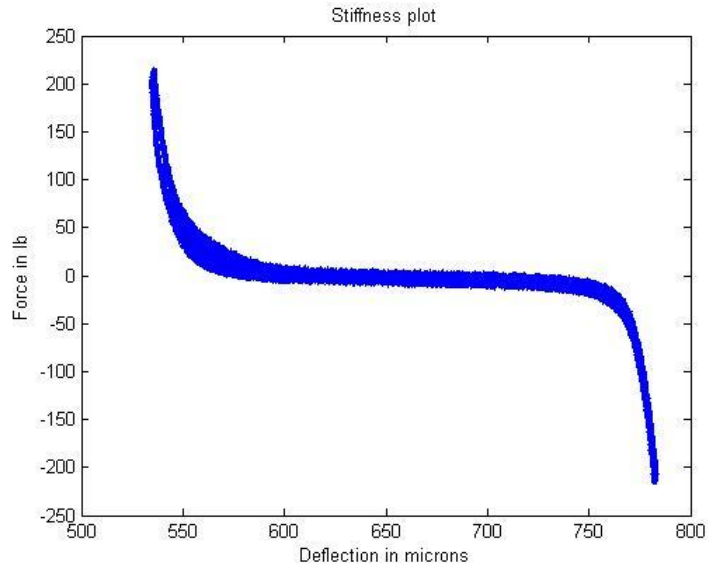


Figure 5-2 Stiffness Plot with 0.008" shim

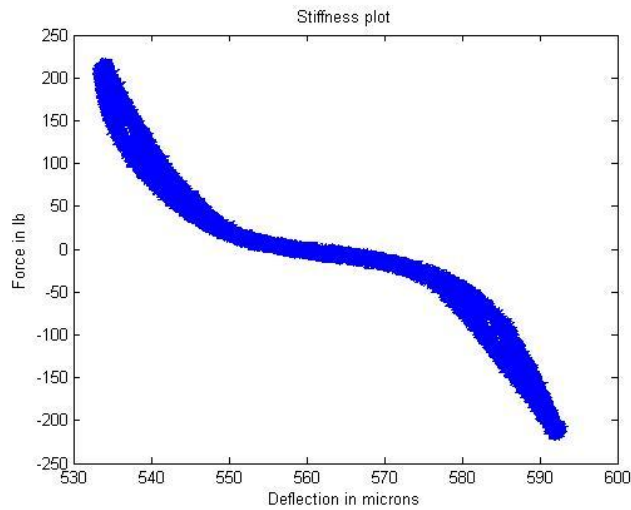


Figure 5-3 Stiffness plot without shim.

Structural stiffness is measured by taking the slope of force against deflection, the structural stiffness is measured using shim and without shim. The shim height used was 200 microns. The structural stiffness of the Rayleigh step bearing was measured by

push pull mechanism as shown in Figure 5-1. The structural stiffness of the bearing with shim is 34MN/m and without shim is 35MN/m.

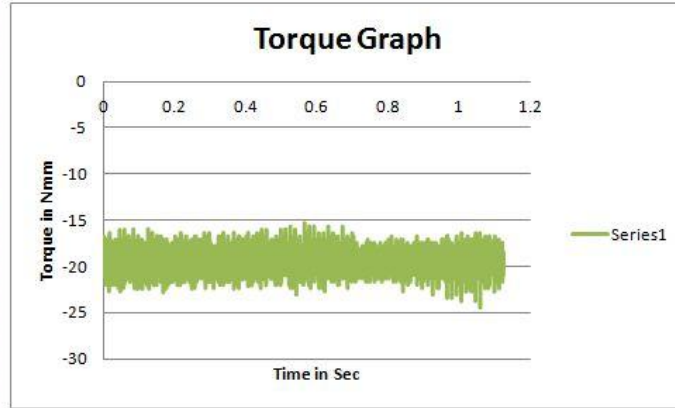


Figure 5-4 Torque Graph

Figure 5-4 shows a torque graph. The torque signal is generated by dynamic load cell which is connected to torque rod, the test rig is run at 15,000 rpm and various parameters are measured. Figure 5-5 and 6 shows the axial load signal and temperature profile running at 15,000 rpm.

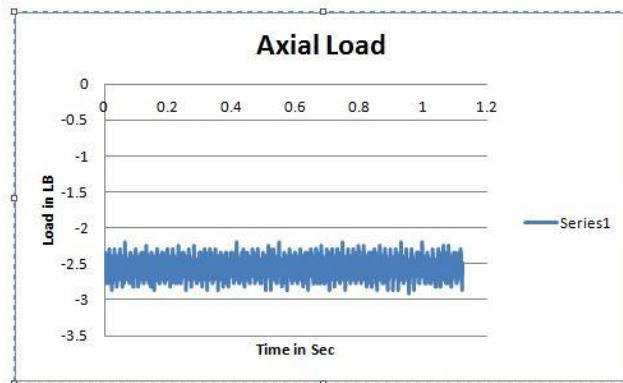


Figure 5-5 Axial load Graph

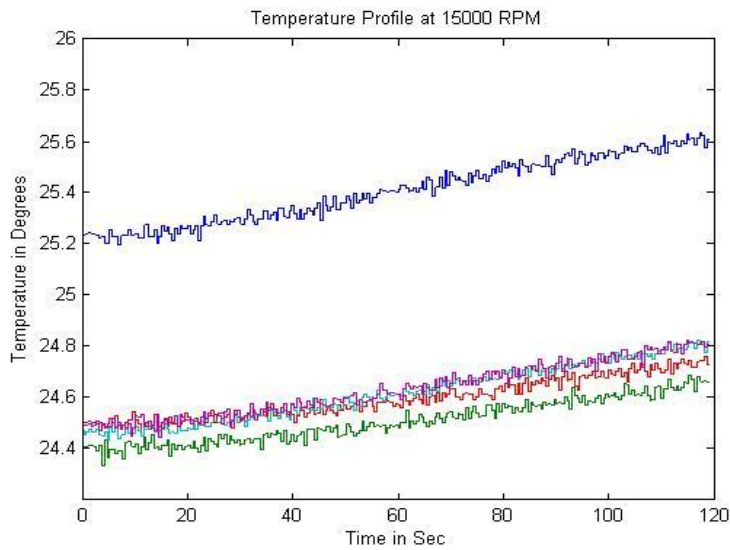


Figure 5-6 Temperature Graph

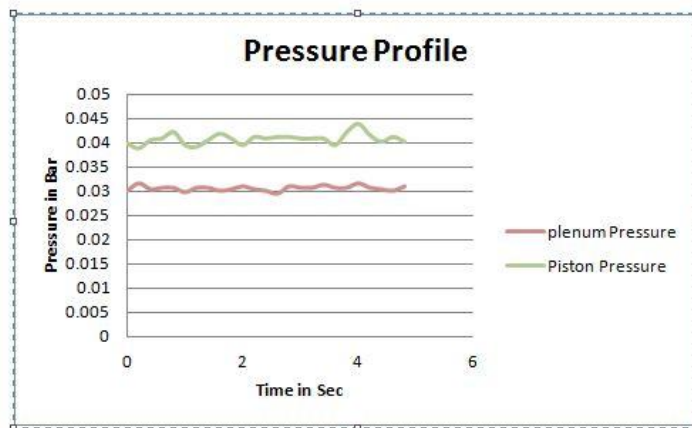


Figure 5-7 Pressure Profile

### Conclusion

The experimental results are few for air foil thrust bearings due to the challenges in design, manufacturing and assembly. Hence it is essential to develop a test rig which will monitor various parameters of air foil thrust bearing. The scope of this research is to develop an air foil thrust bearing test rig which is capable of producing results for torque,

axial load, temperature and pressure. An air foil thrust bearing is designed, manufactured and assembled for which stiffness is evaluated based on push pull mechanism.

The rig developed can efficiently measure torque, temperature and pressure. The rig requires fine tuning in clearance between thrust pad and thrust runner before it can run for several hours to test torque, load, temperature and pressure.

#### 5.1 Future Work

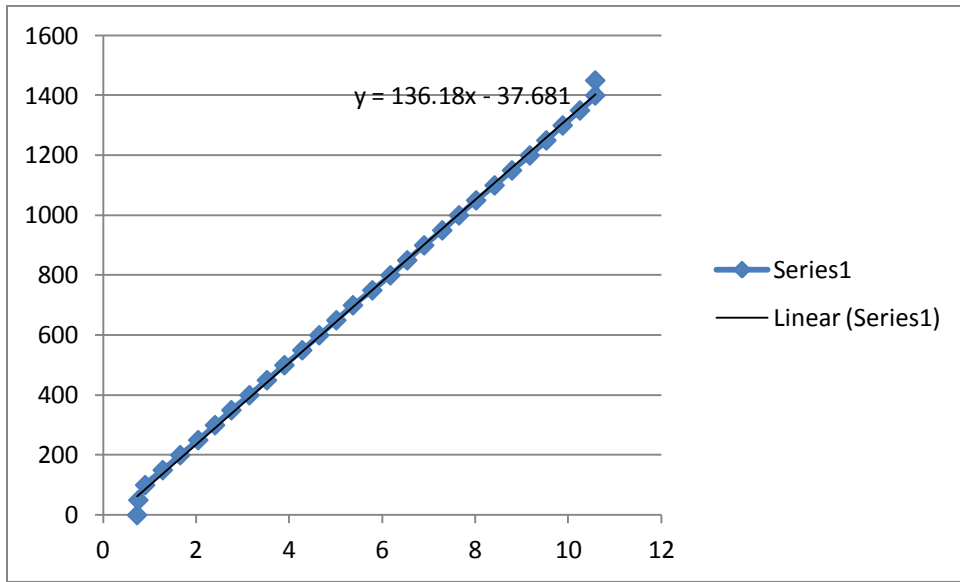
Alignment is an important issue during set up, hence selecting a coupling is an important factor. Using magnetic coupling it will help in alignment, as it can self align with shaft. The balance piston has too much leakage that can be fixed by improving balance piston clearance.

## Appendix A

### Proximity Calibration to measure Stiffness

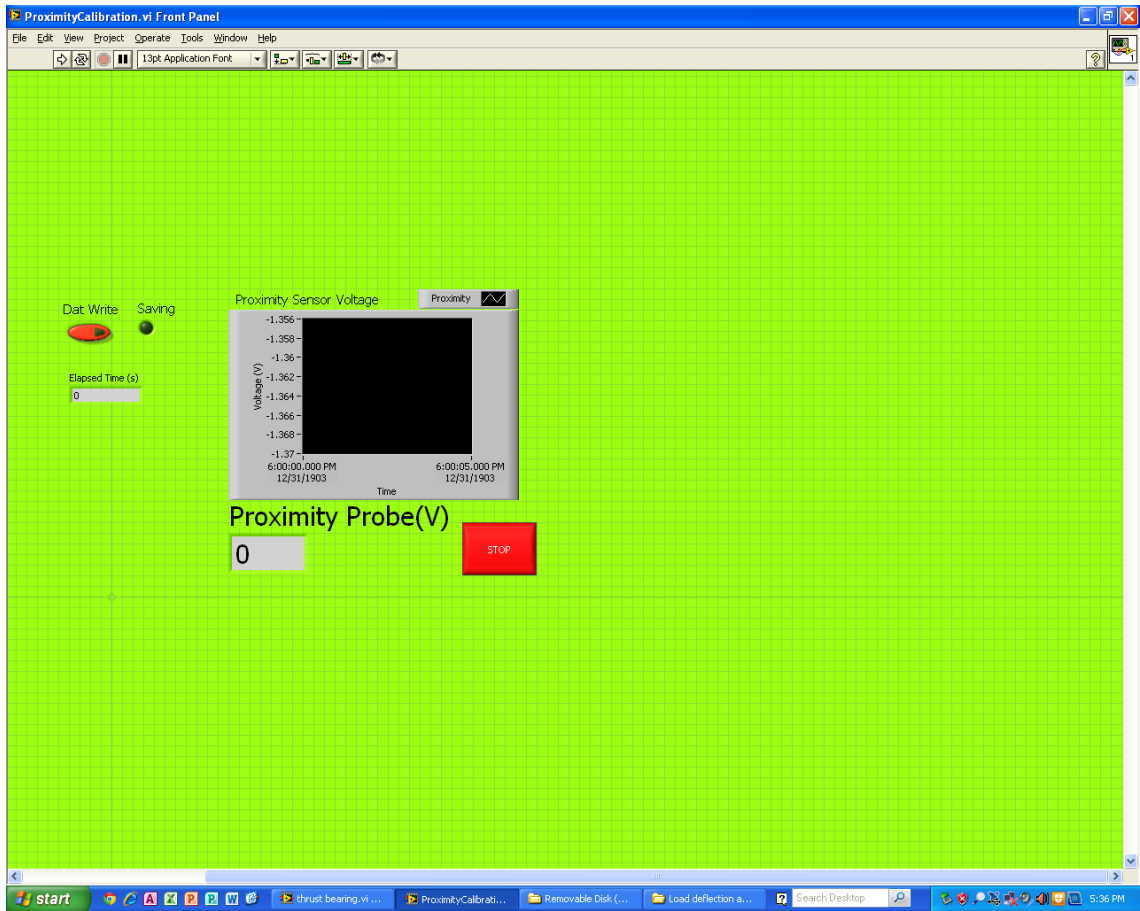


Thrust runner displacement is measured by the difference in distance measured by two proximity probe from their initial position. Two probes are calibrated against their respective surfaces, one probe is calibrated against the back plate surface on which test thrust bearing is mounted another probe is installed on the piston and is calibrated against the shaft.

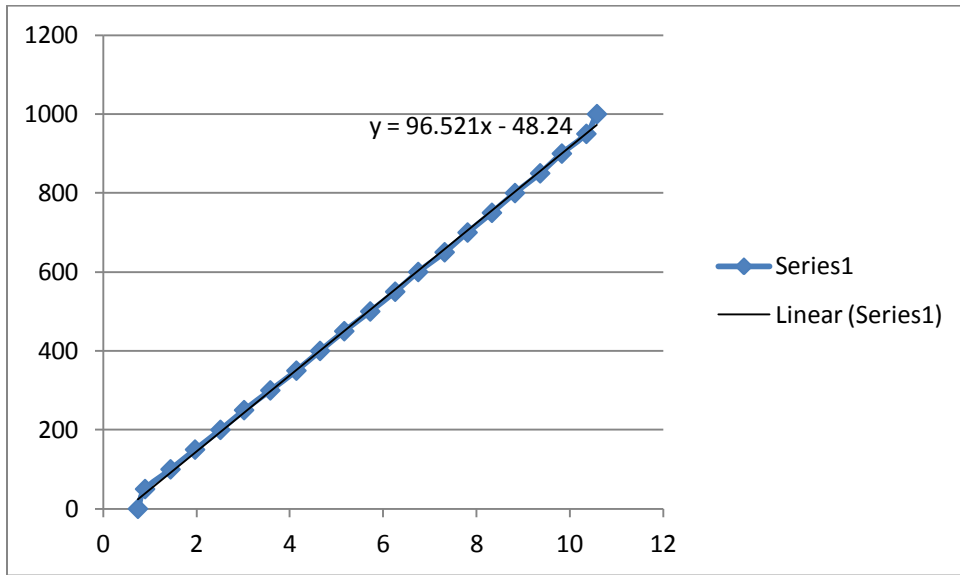


A-0-1 Probe Calibration of Back Plate

The above figure is the probe calibration graph against the back plate of the test thrust bearing. To measure the displacement by the probe, the gain and offset of the probe against the particular surface is required. Hence by the graph gain and offset of the probe against the surface is determined. Second probe is calibrated against the shaft surface; the probe is installed on the piston which determines the displacement of shaft. Therefore, calculating the distance moved by the probes from their initial point thrust runner displacement is determined. Using a LabView VI as shown in the Figure A-0-2 displacement of the probe can be measured. The calibration graph for the second probe can be seen in Figure A-0-3.



A-0-2 Probe Calibration VI



A-0-3 Probe Calibration graph piston end

## Bibliography

- [1] Dykas, B., Bruckner, R., DellaCorte, C., Edmonds, B., and Prah, J., 2008, "Design, Fabrication, and Performance of Foil Gas Thrust Bearings for Microturbomachinery Applications," ASME Turbo Expo 2008, Berlin, Germany, June 9-13, ASME Paper number GT2008-50377.
- [2] Heshmat, H., Walowit, J. A., and Pinkus, O., 1983, "Analysis of Gas Lubricated Compliant Thrust Bearings," ASME Journal of Lubrication Technology, **105**(4), pp. 638-646.
- [3] Brian Dykas, 2006, *Factors Influencing the Performance of Foil Gas Thrust Bearings for Oil-Free Turbomachinery Applications*, Phd thesis, Case Western Reserve University.
- [4] Lee, D., and Kim, D., 2011, "Design and Performance Prediction of Hybrid Air Foil Thrust Bearings," ASME Journal of Engineering for Gas Turbines and Power, **133**(4), pp. 042501 (13 pages); doi:10.1115/1.4002249.
- [5] Robert Dickman. 2010, *An Investigation of Gas Foil Thrust Bearing Performance and its Influencing Factors* , Masters thesis, Case Western Reserve University.
- [6] Anonymous 2005, "MiTi Developments," , **22**.
- [7] Kim, D., 2011, "Tribology Notes," .
- [8] Lee, D., and Kim, D., 2011, "Three-Dimensional Thermo-Hydrodynamic Analyses of Rayleigh Step Air Foil Thrust Bearing with Radially Arranged Bump Foils," STLE Tribology Transaction, **54**(3), pp. 432-448.

### Biographical Information

Rohit Harishchandra Yadav graduated in May 2009 with Bachelors in Mechanical Engineering from University of Mumbai. He worked as a project manager for a year for a logistic company. After working for a year he came to pursue masters in mechanical engineering from University of Texas at Arlington at Fall 2010.